

Open Research Online

The Open University's repository of research publications and other research outputs

Thickness characteristics of phoehoe lavas in the Deccan Province, Western Ghats, India, and in continental flood basalt provinces elsewhere

Journal Item

How to cite:

Mittal, Tushar; Self, Stephen and Jay, Anne (2021). Thickness characteristics of phoehoe lavas in the Deccan Province, Western Ghats, India, and in continental flood basalt provinces elsewhere. *Frontiers in Earth Science - Volcanology* (In Press).

For guidance on citations see [FAQs](#).

© 2020 Tushar Mittal; 2020 Stephen Self; 2020 Anne Jay



<https://creativecommons.org/licenses/by-nc-nd/4.0/>

Version: Submitted Version

Link(s) to article on publisher's website:

<http://dx.doi.org/doi:10.3389/feart.2020.630604>

Copyright and Moral Rights for the articles on this site are retained by the individual authors and/or other copyright owners. For more information on Open Research Online's data [policy](#) on reuse of materials please consult the policies page.

Thickness characteristics of pāhoehoe lavas in the Deccan Province, Western Ghats, India, and in continental flood basalt provinces elsewhere

Stephen Self^{1*}, Tushar Mittal¹, Anne E. Jay²

¹University of California, Berkeley, United States, ²The Open University (United Kingdom), United Kingdom

Submitted to Journal:
Frontiers in Earth Science

Specialty Section:
Volcanology

Article type:
Original Research Article

Manuscript ID:
630604

Received on:
18 Nov 2020

Revised on:
14 Dec 2020

Journal website link:
www.frontiersin.org

Conflict of interest statement

The authors declare that the research was conducted in the absence of any commercial or financial relationships that could be construed as a potential conflict of interest

Author contribution statement

SS is responsible for the writing, field data collection, and formulation of the study. TM is responsible for the data compilation, data analysis, as well as contribution to the writing and analysis. AEJ contributed to the formulation, writing, as well as field data collection.

Keywords

Continental flood basalt provinces, Deccan Traps, Columbia River Basalts, Pāhoehoe, Flow-field, sheet-lobe, hummocky pāhoehoe lavas

Abstract

Word count: 319

We provide the first global compilation of pāhoehoe lava-lobe thicknesses from various continental flood basalt provinces (~ 3800 measurements) to compare characteristic thicknesses within and between provinces. We refer to thin lobes (≤ 5 m), characteristic of “compound” lavas, as hummocky pāhoehoe lava flows or flow-fields. Conversely, we term thicker lobes, characteristic of “simple” flows, as coming from sheet-lobe-dominated flows. Data from the Deccan Traps and Columbia River flood-basalt provinces are archetypal since they have the most consistent datasets as well as established chemo- and litho-stratigraphies. Examining Deccan lobe thicknesses, we find that previously suggested (and disputed) distinct temporal and regional distributions of hummocky pāhoehoe and sheet-lobe-dominated flow fields are not strongly supported by the data and that each geochemically-defined formation displays both lobe types in varying amounts. Thin flow-lobes do not appear to indicate proximity to source. The modal lobe thickness of Deccan formations with abundant “thin” lava-lobes is 8m, while the mode for sheet-lobe-dominated formations is only 17m. Sheet-lobes up to 75-80m are rare in the Deccan and Columbia River Provinces, and ones > 100m are exceptional globally. For other flood basalt provinces, modal thickness plots show a prevalence towards similar lobe thicknesses to Deccan, with many provinces having some or most lobes in the 5-8m modal range. However, median values are generally thicker, in the 8-12m range, suggesting that sheet-lobes dominate. By contrast, lobes from non-flood basalt flow-fields (e.g., Hawai‘i, Snake River Plain) show distinctly thinner modes, sub-5m. Our results provide a quantitative basis to ascertain variations in gross lava morphology and, perhaps, this will in future be related to emplacement dynamics of different flood basalt provinces, or parts thereof. We can also systematically distinguish outlier lobes (or regions) from typical lobes in a province; e.g., North American CAMP lava-lobes are anomalously thick and are closely related to feeder-intrusions, thus enabling a better understanding of conditions required to produce large-volume, thick, flood basalt lava-lobes and flows.

Contribution to the field

We provide the first global compilation of pāhoehoe lava-lobe thicknesses from various continental flood basalt provinces (~ 3800 measurements) to compare characteristic thicknesses within and between provinces. Our results provide a quantitative basis to ascertain variations in gross lava morphology and, perhaps, this will in future be related to emplacement dynamics of different flood basalt provinces, or parts thereof. A quantitative analysis is necessary to estimate the average or typical lava-body thicknesses reported from CFB provinces and systematically compare differences (if any) between provinces. We address these challenges by comparing lava flow morphology (with a clearly defined terminology) across multiple CFB provinces and modern analogs with a specific focus on the Deccan Traps. The global mode for lobe thickness of pāhoehoe sheet-lobes in CFB provinces is in the range 15-20m. The similarity of lobe thickness range for many CFB provinces underlines the similarity of processes on-going during the emplacement of these lava flow-fields, both worldwide and throughout geologic time. Furthermore, it probably also reflects the exceptionally low slopes across active LIPs. With many formations in CFB provinces displaying a range of lobe thicknesses and having hummocky-pāhoehoe-type lobes and units, it is difficult to generally accept emplacement-related criteria, e.g., closeness to vents, based on lobe characteristics.

Funding statement

From the submitted ms:

S. Self acknowledges funding support from NSF EAR-1615021 and the Esper S. Larsen Fund of the University of California, Berkeley. T. Mittal acknowledges graduate funding support from the NSF grant EAR #1615203 and the Crosby Postdoc Fellowship at MIT. AEJ

has been supported by The Open University (UK), a NERC (UK) studentship, and the Daphne Jackson Trust.

Ethics statements

Studies involving animal subjects

Generated Statement: No animal studies are presented in this manuscript.

Studies involving human subjects

Generated Statement: No human studies are presented in this manuscript.

Inclusion of identifiable human data

Generated Statement: No potentially identifiable human images or data is presented in this study.

Data availability statement

Generated Statement: The datasets presented in this study can be found in online repositories. The names of the repository/repositories and accession number(s) can be found below: The lava lobe thickness datasets used in this study are provided as Supplementary files with the manuscript along with Jupyter Notebooks for data analysis as well as various analysis plots for each CFB dataset at: <https://figshare.com/s/55fab1e83524e6184fd5>" (we will add a DOI for the final accepted manuscript).

In review

1 **Thickness characteristics of pāhoehoe lavas in the Deccan Province,**
2 **Western Ghats, India, and in continental flood basalt provinces**
3 **elsewhere**

4 **Stephen Self¹, Tushar Mittal^{1,2}, and Anne E Jay³**

5 ¹Earth and Planetary Science Department, University of California, Berkeley, CA, USA.

6 ²Department of Earth, Atmosphere and Planetary Sciences, Massachusetts Institute of Technology,
7 Cambridge, MA, USA

8 ³School of Environment, Earth, Ecosystem Sciences, The Open University, Walton Hall, Milton
9 Keynes, MK7 6AA, UK

10 *** Correspondence:**

11 Stephen Self

12 sself@berkeley.edu

13 **Keywords: Continental Flood Basalt Provinces, Deccan Traps, Columbia River Basalts,**
14 **pāhoehoe, flow-field, sheet-lobe, hummocky pāhoehoe lavas.**

15 **1. Abstract**

16 We provide the first global compilation of pāhoehoe lava-lobe thicknesses from various continental
17 flood basalt provinces (~ 3800 measurements) to compare characteristic thicknesses within and
18 between provinces. We refer to thin lobes ($\sim \leq 5\text{m}$), characteristic of “compound” lavas, as hummocky
19 pāhoehoe lava flows or flow-fields. Conversely, we term thicker lobes, characteristic of “simple”
20 flows, as coming from sheet-lobe-dominated flows. Data from the Deccan Traps and Columbia River
21 flood-basalt provinces are archetypal since they have the most consistent datasets as well as established
22 chemo- and litho-stratigraphies. Examining Deccan lobe thicknesses, we find that previously suggested
23 (and disputed) distinct temporal and regional distributions of hummocky pāhoehoe and sheet-lobe-
24 dominated flow fields are not strongly supported by the data and that each geochemically defined
25 formation displays both lobe types in varying amounts. Thin flow-lobes do not appear to indicate
26 proximity to source. The modal lobe thickness of Deccan formations with abundant “thin” lava-lobes
27 is 8m, while the mode for sheet-lobe-dominated formations is only 17m. Sheet-lobes up to 75-80m are
28 rare in the Deccan and Columbia River Provinces, and ones $> 100\text{m}$ are exceptional globally. For other
29 flood basalt provinces, modal thickness plots show a prevalence towards similar lobe thicknesses to
30 Deccan, with many provinces having some or most lobes in the 5-8m modal range. However, median
31 values are generally thicker, in the 8-12m range, suggesting that sheet-lobes dominate. By contrast,
32 lobes from non-flood basalt flow-fields (e.g., Hawai’i, Snake River Plain) show distinctly thinner
33 modes, sub-5m. Our results provide a quantitative basis to ascertain variations in gross lava
34 morphology and, perhaps, this will in future be related to emplacement dynamics of different flood
35 basalt provinces, or parts thereof. We can also systematically distinguish outlier lobes (or regions) from

36 typical lobes in a province, e.g., North American CAMP lava-lobes are anomalously thick and are
37 closely related to feeder-intrusions, thus enabling a better understanding of conditions required to
38 produce large-volume, thick, flood basalt lava-lobes and flows.

39 2. Introduction:

40 Continental flood basalt (CFB) province emplacement represents some of the largest volcanic events
41 in Earth history, associated with the biggest (up to or perhaps > than 5,000 km³; Self et al., 2014) and
42 longest (~ 1000 km; Self et al., 2008) recognized lava flow-fields on Earth. Although flood basalt lava
43 flows have been studied extensively for decades, we still lack a good understanding of some
44 fundamental aspects of lava flow emplacement, such as typical eruptive fluxes. Lava flow morphology,
45 especially flow thickness, is a fundamental characteristic of CFBs that is potentially linked to lava-
46 flow eruptive rates (e.g., Bondre et al., 2004). Thus, analysis of lava flow morphology can help examine
47 the spatial and temporal variations in the emplacement rate of a CFB province. These spatiotemporal
48 eruptive rate variations are critical for understanding the magmatic plumbing systems of CFBs (Ernst
49 et al. 2019, Sheth and Cañón-Tapia, 2015) as well as the environmental impacts (e.g., Schmidt et al.,
50 2016; Hull et al. 2020, Clapham & Renne 2019, Landwehrs et al. 2020).

51 However, studying lava flow morphology for CFB flows is challenging for a variety of reasons.
52 First, the morphology and physical form of lava flows may change across and within different
53 formations in CFB provinces as well as chronologically throughout the emplacement of a CFB (Passey
54 and Bell, 2008, Kale et al., 2020a). Thus, any analysis needs to carefully account for these effects.
55 Second, most previous CFB studies provide only a qualitative description of morphology or are focused
56 on a single outcrop or region. Consequently, it is not easy to quantify any spatio-temporal variations
57 between different morphological styles. Furthermore, consistent terminology is essential to accurately
58 compare flow morphologies over 100s of km and across CFBs. Finally, in field geology, the eye is
59 always drawn to the extremes, be they small or large. Thus, a quantitative analysis is necessary to
60 estimate the average or typical lava-body thicknesses reported from CFB provinces and systematically
61 compare differences (if any) between provinces.

62 We address these challenges by comparing lava flow morphology (with a clearly defined
63 terminology) across multiple CFB provinces and modern analogs with a specific focus on the Deccan
64 Traps (henceforth Deccan). A simple expression of flow morphology is lava-lobe thickness, as this
65 represents the essential morphological difference reported from CFB pāhoehoe (phh) lavas – sheet-
66 lobe-dominated (simple) vs. hummocky-lobe-dominated (compound) lavas (e.g., Walker, 1971;
67 Bondre et al., 2004; Sheth, 2006; Jay et al., 2018). The thickness of lobes or flows is also perhaps the
68 only physical property of basalt lavas consistently reported across many studies. We first describe our
69 volcanological terminology for CFB flows (in Section 2) following Self et al. (1998) and Thordarson
70 and Self (1998). Within our terminology, thin (<5m) lobes can be equated to hummocky-lobe-
71 dominated flows and thicker (>5m) lobes to sheet lobe-dominated flows. It is important to note that
72 lava flow-fields are, to some extent, always compound (e.g., Vye-Brown et al. 2013). Thus, the
73 influence of typical CFB province outcrop scales (an approximately 2D slice of a large 3D flow
74 structure) on interpreting whole lava flow-fields and typical province-wide lobe thicknesses requires
75 careful attention.

76 We then present lava lobe thickness data based on logs made through flood-basalt lava
 77 sequences from which we can estimate the value and range of lobe thicknesses for each formation (or
 78 sometimes sections) and whole CFB provinces. Data are presented first for the Deccan Volcanic
 79 Province (Deccan) (**Figure 1A**), with most information coming from the Western Ghats (Sahyadri)
 80 where the geochemical stratigraphy is well-understood (e.g., Subbarao, 1999; Kale et al., 2020a and b).
 81 The relationship of typical lobe thicknesses amongst the various geochemical formations provides
 82 important insights into the changing style of eruption of typical Deccan units as the main lava pile grew
 83 during its ~ 1 Ma lifetime (Sprain et al., 2019, Schoene et al. 2019). Our work also makes it possible
 84 to test and quantify the suggestions of Deshmukh (1988) and Walker (1971, 1999) that smaller
 85 "compound" lava lobes dominate in the northern areas of the main Deccan province and that thicker
 86 "simple" flows occur more commonly to the south and east (**Figure 1C**). This observation was
 87 interpreted as being indicative of a lava morphology change due to changing distance from source.
 88 Although the idea has been disputed by others (Bondre et al. 2004; Self et al. 2006; Jay et al., 2018),
 89 our new dataset can help further quantitatively test this hypothesis. Next, we compile lobe thickness
 90 measurements from other CFB provinces (for a total of ~ 3800 individual measurements) from multiple
 91 studies. In concert with other studies (e.g., Bondre et al., 2004, Duraiswami et al., 2017, Jay et al.,
 92 2018) our results help illustrate the variety in a specific morphological lava feature (lobe thickness),
 93 both within a single CFB formation and for entire CFB provinces. Additionally, we can possibly use
 94 lobe thickness distributions to quantitatively compare and group together various CFBs with similar
 95 flow emplacement dynamics. This analysis thus provides a framework to generalize results from
 96 individual well-studied CFB sections, such as the Columbia River Basalts (CRB, e.g., Vye-Brown et
 97 al., 2013), to other CFB lava flow-fields.

98 3. Physical features of lava flows – Terminology

99 Since observations show that 'a'ā flows (*sensu lato*) seem to be exceedingly rare in most CFB
 100 provinces, including the Deccan (Brown et al., 2011), and despite some reports to the contrary (e.g.,
 101 Duraiswami et al., 2014), we will focus only on phh lava flow fields. The occasional 'a'ā lobe in a phh
 102 flow-field is not unexpected. We use *flow-field* (see Self et al., 1997, after Kilburn and Lopes, 1991)
 103 as a convenient term for the entire products of one effusive eruption, be it a CFB lava eruption or a
 104 much smaller one. We use the term (*inflated*) *lava sheet-lobe* (as per Self et al., 1997; Self et al., 1998;
 105 Thordarson and Self, 1998), shortened to *sheet-lobe (SL)*, to describe widespread lava bodies
 106 surrounded by lava crusts. Note that this category would include a number of the transitional flow types
 107 such as the rubbly pāhoehoe flows reported in Deccan Traps (e.g., Duraiswami et al., 2017) as well as
 108 modern basaltic eruptions (Laki – Guilbaud et al. 2005). These bodies are much more extensive in the
 109 horizontal than the vertical axis-and are mostly $\geq 5\text{m}$ in total thickness. In CFB provinces these lobes
 110 are seen only in 2-D exposures (e.g., **Figure 2A, B and C**) and are equivalent to lava bodies called
 111 "simple", although Walker (1971), in defining this term, wrote:

112 *In consequence, he [Walker] doubts if simple basalt flows occur at all, although simple*
 113 *andesite, dacite, rhyolite and trachyte flows do appear to exist. The application of the terms simple,*
 114 *compound, and multiple to basalt is probably most useful for older lavas which belong to dissected*
 115 *volcanic piles and are therefore not seen in their entirety; the terms are most usefully used in a*

116 *descriptive way to convey the character of a flow as seen in a particular cross-section. If the average*
 117 *basalt lava flow were seen in its entirety it would prove to be compound and locally multiple in*
 118 *character, though over much of its extent it might be made of a single unit.*

119 We thus use sheet-lobe(s) for what have been called simple flows in outcrop (**Figure 2A**). We
 120 use *hummocky pāhoehoe* (HP, Swanson, 1973; Hon et al., 1994) for what have been called compound
 121 phh flows in outcrop (made of several to many small lava lobes, **Figure 2C**), and we suggest that lobes
 122 of < and > 5m thickness is a convenient divide for distinguishing HP lavas from SLs, in CFBs at least.
 123 We find that the lobes in HP-dominated flow sequences are usually < 5 m and show only nascent
 124 internal structure of the type shown on **Figure 2A**. We would note that SLs considerably thinner than
 125 3 m exist in the lava flow-field of the recent (1983-2018) eruption on Kīlauea, Hawai‘i (Sharma et al.,
 126 2000, see our **Figure 2A**); these possess all features of much thicker SLs, but they are not of concern
 127 to this paper. The internal structure of SLs (**Figure 2A**) is also different and more variably developed
 128 than that of many HP lobes, and the internal structure is used to distinguish the top and bottom crusts
 129 of lava lobes.

130 4. Datasets

131 4.1 Logs from field work and, occasionally, drillcores

132 We obtained lava lobe thickness data from detailed volcanological logs made through lava piles in
 133 CFB provinces largely using exposures along road cuts (and rail-road cuts) but also in natural cliffs
 134 and slopes, and, occasionally, streambeds and drill cores. Lobe thickness data from the Deccan were
 135 measured by Jay (2005) and reported in Jay et al. (2009) for a total of ~ 5km of lava flows across
 136 multiple transects (see **Figure 1B**, for location of the logged transects). Complementary paleomagnetic
 137 and geochemical work was done on lava samples from these Deccan traverses (as well as
 138 geochronology; Renne et al., 2015; Sprain et al., 2019). Thus, given the current geochemical
 139 stratigraphic framework (**Figure 3B**, Beane et al., 1986; Jay and Widdowson, 2004), we can clearly
 140 assign each flow lobe to a geochemical formation. We have similar logs for the CRB and Karoo flood
 141 basalt provinces (Jay et al. 2018, Moulin et al. 2017), collected by the authors. For the Deccan and
 142 Karoo, the logs are exemplified by those in **Figure 3A** (**Supplementary Figure 1**, see also Figure 4 in
 143 Jay et al., 2009 and 2016). Data also exists from drill-hole cores in the Koyna region of the Western
 144 Ghats, part of the Deccan where scientific drill-holes were drilled (Sinha et al., 2017; Mishra et al.,
 145 2017), as well as the Killari Scientific Drill Hole (Gupta et al., 2003, Kumar et al. 2010). In order to
 146 extend the spatial coverage to other Deccan sub-provinces besides the Western Ghats, we also include
 147 previously published sections from the north-western Deccan (Peng and Mahoney, 1995), Narmada-
 148 Tapi Rift Zone region (Mahoney, 2000; Tejankar, 2003; Doke, 2013), Malwa Lobe
 149 (Kasiviswanandham, 2003), and Mandla Lobe (Sengupta and Ray, 2006; Pathak et al. 2017).

150 For the CRB province, data are from Thordarson and Self (1998) and Vye-Brown et al. (2013)
 151 including various unpublished measurement by the authors using the same logging principles as the
 152 abovementioned studies. Data from the nearby Snake River Plain basalts, included as an example of a
 153 “plains”-type basalt province (mini-CFB, after Greely 1982), are from a deep drill-hole core reported

154 by Potter et al. (2019). Criteria for distinction of flow-lobes in that core is described by the authors (*et*
155 *seq.*, pgs 3-8) and are like those employed by us, allowing a consistent lobe delineation.

156 We also include similar datasets for other CFBs from a few studies (see **Supplementary**
157 **Dataset 1**) while ensuring that the flow lobe definition used in these studies is as consistent as possible
158 with our terminology. The provinces are Central Atlantic Magmatic Province (CAMP), Ethiopian flood
159 basalts, Emeishan flood basalts, the Siberian Traps, the North Atlantic Magmatic Province (NAMP;
160 mainly the Faroe Islands and Greenland), the Big Island of Hawai'i (for purposes of comparison), and,
161 briefly, Ontong Java Plateau, to include an oceanic LIP. For all provinces with data on lobes, we have
162 followed the assigned stratigraphic nomenclature of the lava flow-fields or formations from the
163 respective studies.

164 4.2 Quality of data and caveats

165 Lobe thicknesses were measured from the top of each upper lava crust to the bottom of the lower crust
166 (**Figure 2A**) ignoring any soil and /or weathering-induced lava rubble at top or bottom but including
167 altered flow-tops (usually vesicular). SL lateral extents are not reported in this work and knowledge of
168 these is sparse. The thickness of any small and/or thin precursor or breakout lobes associated with SLs
169 were measured separately and the data included as independent lava lobes. The main challenge when
170 measuring thicknesses of lava lobes is to capture the full range of lobe sizes. In our logs, we measured
171 the thicknesses of small HP-type lobes on a few characteristic lobes and the thickness of the whole HP-
172 dominated part of the sequence. Although this provides a first-order estimate of HP lobes and small-
173 lobe-dominated portions of SLs, we anticipate that small lobes are overall likely under-reported in our
174 analysis. We also note that the thickest lobes are rarely completely exposed due to limited outcrop size
175 and/or accessibility (e.g., as at Arthur's Seat in the Deccan (**Figure 2B** and **Supplementary Figure**
176 **1**), and that the thinnest lobes occur in such abundance that measuring a significant thickness of lava
177 lobe-by-lobe is a daunting task. Moreover, piles of thin lobes are often severely weathered. We thus
178 realize that in plots of numbers of lobes of various thicknesses, both the extremes in size are not as
179 well represented as the middle parts of the size distribution.

180 In our Deccan dataset, flow lobes < 2m were measured by hand using a tape measure and the
181 thicknesses are good to +/- ~ 10 cm (1 cm for the thinnest lobes). For thicker lobes, the thickness was
182 calculated using a barometric altimeter for each individual sheet lobe using the elevation at the top and
183 bottom of each lobe. This choice helps minimize any errors due to instrument drift throughout the day
184 due to changing temperature. Given the lack of accurate topographic maps, we anchored the elevation
185 of the top, bottom, and middle of each traverse, such as Ambenali Ghat, using a differential GPS which
186 we left running for up to 3 hours. Almost all lobes reported are complete, but we did measure a few
187 partial lobes to capture the highest end of the thickness spectrum. In these cases, virtually the whole
188 lobe was measurable, and the sparse number is not expected to make a difference to the top end of the
189 reported thickness spectra for the Deccan, Karoo, or CRB data sets.

190 We find no significant statistical difference between data obtained from surface exposures vs
191 that from cores drilled through the lava piles (when comparing results from the same geochemical

192 formations), even though traverses through surface-exposed lava piles often stretch for many
 193 kilometers laterally (**Figure 1B**).

194 **5. Results - Lava body thicknesses**

195 Lava-lobe thickness data from the Deccan are plotted in various ways; we give more details on the
 196 Deccan set as all others follow with similar plots. The ways are: lobe thicknesses of individual lobes
 197 vs altitude above sea level (as a measure of stratigraphic height); plots of lobe thickness vs number-of-
 198 lobes-in-each-thickness-bin; and also as an univariate kernel density estimator to calculate the
 199 probability density function of lava flow thicknesses in a data set. This latter plot gives an immediate,
 200 useful view of the whole thickness distribution. We also present “violin” plots where the thickness
 201 distribution is represented in the vertical (y) and the number of measured lobes is expressed in the
 202 horizontal (x) axis.

203 5.1 Deccan Volcanic Province including Koyna region

204 Thickness data plotted against elevation, equivalent to stratigraphy in many parts of the 66.4-
 205 65.5 Ma-old Deccan Province (Sprain et al., 2019), including a subdivision of the lava pile into
 206 formations (**Figures 3B and 4A and B**), show that measured Deccan lava lobes vary from < a few m
 207 thick to ~ 90m thick (the latter in the Mahabaleshwar Formation). The stratigraphic subdivision shown
 208 is that for the recognized chemostratigraphic Deccan formations. Although the lithostratigraphic
 209 subdivision (after Godbole et al., 1996) is also used in the literature (e.g., Verma and Khosla, 2019), it
 210 is not as well developed as the chemostratigraphic formations and we thus do not use it for the analysis
 211 here. The plots on **Figure 4A** are arranged by latitude of the traverse (top = N, bottom = S) and the
 212 main weathering horizons (boles) recognized in the lava pile are shown by vertical red lines. The bole
 213 data is by no means complete and no significance should be placed upon it, other than in a first-order
 214 sense (see comments below). Gaps in the data indicate gaps in exposure on the traverses. Further, the
 215 data comes from a small region of the central Western Ghats of western India in Maharashtra State, so
 216 there could be regional bias (**Figure 1B**).

217 One limitation of our present Deccan data is that only one traverse (Matheran) includes the
 218 lowest chemostratigraphic formations (Kalsubai Sub-group). This lack will be addressed in future
 219 work. Nevertheless, it can be seen (**Figure 4A**) that all formations logged have small lobes, and all
 220 formations except Khandala have at least one small-lobe-dominated section. Note that the Ambenali
 221 Ghat traverse covers over twice as much elevation as the others, and this ghat is, in fact, the informally
 222 recognized Western Ghats “type section” on which much work has been based (e.g., Beane et al., 1986;
 223 Mahoney et al., 1982; Chenet et al., 2008; Jay et al., 2009). Thicknesses of lobes within and among
 224 formations do not vary greatly, with all formations except Neral, Bhimashankar, and Khandala having
 225 lobes at least 40 m thick. Based on our two traverses that include significant Kalsubai (lowest) and
 226 Lonavala (middle) Sub-group lava sequences (Matheran and Varandah Ghats), there appears to be a
 227 slight prevalence for small-lobe-dominated (or hummocky phh) lavas in those formations, in
 228 accordance with previous studies (e.g., Bondre et al., 2004).

229 **Figure 4B** plots lava lobe thicknesses mainly from the Wai Formation in the same scheme as
230 **Figure 4A** to examine possible lobe thickness variations over 80 km distance from N to S. No strong
231 pattern of variation is evident, yet southward could be more distal from some suggested sources areas
232 (Vanderkluyzen et al., 2011). We also see that the altitude of the Ambenali-Mahabaleshwar contact
233 varies by more than 50 m in a relatively small region (also see **Figure 2C**) thus illustrating that using
234 altitude for large scale correlation is potentially problematic.

235 Furthermore, we can use the Ambenali-Mahabaleshwar contact height and the location of
236 Chron 29N-Chron 29R transition as well characterized time tie-points to assess whether flow lobe
237 characteristics (number, thickness, small-lobe-dominated fraction) are spatially variable. We find that
238 among sections, the number of flow lobes varies from 2-5 with thicknesses ranging from 5 m to 35 m
239 with some sections having small-lobe-dominated flows (e.g., Kelgar, Tapola, Wai-Panchgani) while
240 others do not (e.g., Ambenali Ghat, Khumbarli Ghat). There is no clear relationship between flow lobes
241 in individual sections which suggest that lava flow morphology characteristics can significantly vary
242 over small spatial distances (compared to the scale of the overall CFB province). A mild southerly dip
243 to the lava pile of 0.5 to 1 degree in the study area (Mitchell and Widdowson, 1991) explains why the
244 older formations appear in the north and why stratigraphically higher formations occur at progressively
245 lower elevations southward. The types of lavas plotted in **Figure 4B** can be seen in the logs in
246 **Supplementary Figure S1**.

247 The whole range and modes of lobe thickness in each Deccan formation (**Figure 5A**) and sub-
248 group (**Figure 5B**) are shown as univariate kernel density estimators to calculate the probability density
249 function (PDF) of lava flow thicknesses in a data set. In these plots the thickness is plotted against the
250 PDF and the area under the curve totals to 1; the range and mode of the PDF is conveniently seen, and
251 the formations or sub-groups can be easily compared. The number of lobe occurrences in each
252 thickness bin is plotted on the y axis. The “thick tail” of the PDF represents the thickest SLs.
253 Formations with bimodal plots, such as the Bushe, appear to have a mode in the HP range and another
254 in the SL range. We find that all formations, bar one, have lobes covering the whole range of thickness
255 up to 30 m, and one formation (Mahabaleshwar) covers the entire range up to 90 m (see also **Figure**
256 **4**). The Bhimashankar Formation, which is very thin (~ 35 m in the Matheran traverse, **Figure 4A**) and
257 composed of only a few lobes, is the exception having a maximum SL thickness of 14 m (**Figure 5A**).
258 There is clearly a mode in the 20 +/- 5 m range in all formations (except Bhimashankar – measured on
259 one traverse only which is possibly not diagnostic) that represents typical SL sizes with a rarity of
260 much thicker lobes. The smallest lobes, individual precursors to or breakout from SLs and from HP
261 lobes, are in the range of a few m in each formation. Thus, overall, there is only a weak relationship
262 between formation and lobe thickness, which is also explored in later plots. The thickest SLs are
263 generally in the range 50-60 m for the Wai Sub-group and Bushe Formation lavas, but smaller for the
264 others, especially those from the Kalsubai Sub-group, which range around 30-40 m and make up
265 smaller proportions of the PDF.

266 Whole sub-groups of the Deccan have indicative thickness PDFs (**Figure 5B** and **6B**) that
267 support some of the conclusions of previous studies (Bondre et al., 2004), in that the lower, older sub-
268 group (Kalsubai) formations together have the most peaked and thinnest mode, and the upper sub-

269 group (Wai) has the broadest mode with a mean thickness similar to that for the middle sub-group
 270 (Lonavala) formations. This reflects that the Kalsubai subgroup may overall be composed of more HP-
 271 type lava flow fields than the upper two sub-groups but testing the reality and details of this suggestion
 272 require further work. The coarse lobe mode in the Bushe Formation data (**Figure 5A**) suggests that
 273 there may be a genuine bimodal aspect to that formation's thickness characteristics, although more
 274 measurements are needed to confirm this inference.

275 An overall comparison of the Deccan lobe thickness data is seen on a “violin” plot (**Figure**
 276 **6A**), where the lobe thickness variation (y axis) is plotted by the different formations in the various
 277 traverses (x axis). The width of the violin represents the amount of data for each formation and the
 278 thickness range is encapsulated in the vertical distribution. A white dot marks the mean of the
 279 distribution and a black bar the 75th – 25th percentile range. The prevalence of 20-30 m thick SLs is
 280 evident, with the traverse composed of older lavas (Matheran, including Kalsubai and Lonavala Sub-
 281 groups) having slightly smaller means, but not by a marked amount. The plot clearly shows that the
 282 thickest SLs are in the minority in terms of occurrence. Additionally, the figure illustrates that lobe
 283 thickness distribution for a single formation can be variable across different sections further illustrating
 284 the spatially variability of flow morphology in DVP even on a small regional scale.

285 An independent Deccan data set comes from lobe thickness measurements on drill core
 286 obtained from the Koyna area in the Western Ghats (Sinha et al., 2017; Mishra et al., 2017), near to
 287 our Khumbarli Ghat traverse. Although the cored lava formations are not named in these papers, the
 288 local geology suggests they are Wai Sub-group (Duraiswami et al., 2017). The distribution of SL
 289 thicknesses is like our Wai Sub-group data, seen on **Figure 6B**, with a mean and mode around 18-20
 290 m. A maximum reported lobe thickness of 165 m for one lobe in the Koyna cores must be treated with
 291 suspicion as no other lobes of comparable thickness have been found in our work, but it could be real.
 292 We also show lobe thickness distributions from other regions of the Deccan in **Figure 6B**. Killari is
 293 located in the Central Deccan region and is considered part of the eastern extent of the Wai Subgroup
 294 flows (Jay & Widdowson 2008). However, we find that SL thickness is distinctively different from the
 295 Wai lavas with much thicker lobes in the Killari region. This could potentially indicate an effect of
 296 changing flow-lobe thickness with distance from the eruptive center, but we do not have good
 297 constraints on the eruptive locations (Vanderkluyzen et al. 2011, Kale et al. 2020a). By contrast, the
 298 flows in the north-western Deccan (Saurashtra region) are similar to the oldest Western Ghats flows
 299 (Kalsubai group) in terms of lobe thickness (**Figure 6B**). From our data compilation, we find that lava
 300 flows in the northern Narmada-Tapi Rift Zone as well as the Malwa Lobe region have a similar modes
 301 of lobe thickness (~ 20 m thick) to the Western Ghats flows. The flows in this region are most like the
 302 Wai Subgroup flows in terms of their thickness distributions. Finally, the Mandla Lobe flows have
 303 slightly thicker lobes (mode of ~ 25 m) than the Wai Subgroup flows with a distinct lack of thin (< 5m)
 304 lobes.

305 5.2 Karoo continental flood basalt province

306 We use measured sections on three Karoo 182-183 Ma-old CFB province phh lava successions from
 307 Moulin et al. (2017) and Jay et al. (2018), following Figure 4 of the latter reference. The successions

308 are at Naude's Neck, Oxbow, and Moteng Pass. There are no significant differences between lobe-
 309 thickness distributions at each location. Overall, the mean size of lobes appears to be thinner than in
 310 the Deccan. Almost 50 % of the lavas logged by Jay et al. (2018) are HP, a higher proportion than in
 311 any Deccan formation (**Figure 7A vs Figure 4A**). The PDF of the size distributions at the three
 312 locations shows the similarity and mean size of sheet lobes, around 12-15 m: **Figure 7B**). A few SLs
 313 $\sim > 30$ m thick exist, and the violin plots of all locations (**Supplementary Data**) show how similar the
 314 means of the size distributions are, with Naude's Nek lava lobes being a little thinner than the others.

315 5.3 Columbia River Province and Snake River Plain "plains" basalt province

316 Data from the CRB Province are assembled at the formation level for comparison purposes with
 317 thickness data from the Deccan (**Figure 8A**). We present data for the Grande Ronde Basalt and
 318 Wanapum Basalt Formations, the two lava formations emplaced at the climax of CRB volcanism,
 319 between 16.5 and 15.9 Ma ago (Kasbohm and Schoene, 2018; Barry et al., 2010). **Figure 8A** shows
 320 that the PDFs for size distributions of whole formations are quite similar, with a mode at around 15 m
 321 for thin SLs and another mode for thicker SLs in the Grande Ronde. One advantage of displaying CRB
 322 data is that, uniquely in global LIPs, the components are known down to the level of individual flow-
 323 fields. Thus, in **Figure 8A**, we can see that Wanapum Basalt shows quite considerable variation
 324 between the different members comprising the formation: the Roza, Gingko, Sand Hollow, and Palouse
 325 Falls plots are all single flow-fields and are members of the Wanapum Formation; Wallula Corehole
 326 comprises data from several Wanapum members, and Grande Ronde and Wallula Grand Ronde plots
 327 are collective for the Grande Ronde Basalt Formation, and thickness data are quite similar to each
 328 other. **Figure 8B** displays PDFs of the same data as **8A** showing clearly that most CRB data is for SLs,
 329 with HP-thickness lobes in the minority.

330 Lobes in the flow-fields of the Palouse Falls and Sand Hollow eruptions are recognized to be
 331 composed mainly of coarser SLs, while the Gingko flow field has more small SL lobes than most CRB
 332 flows, with Roza lobes falling a little thicker in typical SL size than Gingko (Vye-Brown et al, 2013).
 333 Overall, the PDF plots show that CRB flow-lobes consist of a higher proportion of thicker lobes than
 334 both Deccan and Karoo Provinces (there is a bigger % of the PDF curve under the 30-60 m range). In
 335 other words, the CRB possesses a higher proportion of thicker sheet lobes than the Western Ghats
 336 region of the Deccan but, as such a small part of the Deccan is considered by our data, these claims
 337 may not be sustained after future work.

338 For the Snake River Plain Province lobe thickness data, an example of "plains"-type volcanism
 339 logged in the Kimama borehole by Potter et al. (2019), it is clear (**Figure 8B inset**) that the modal size
 340 of lobes is considerably smaller than in the CRB. In fact, this thick pile of basalt, which accumulated
 341 over ~ 6 Ma, is almost all HP in nature. There is a strong mode in the 2-3 m thickness range and little
 342 of the PDF distribution in the thick range (extending only up to 20m). This contrasts strongly with the
 343 nearby CRB and the Deccan, as expected.

344 5.4 Other CFB provinces and Hawai'i

345 The Deccan, Karoo, and CRB represent our primary data in this study since the datasets were all
 346 collected in a relatively homogeneous manner by the authors. For other CFBs, the data quantity and
 347 quality are more variable. In the following, we discuss compiled data from other provinces in order of
 348 decreasing LIP age using only PDFs of size distributions. As much as possible, we have tried to utilize
 349 a consistent terminology for defining what constitutes a lava lobe based on published stratigraphic logs.

350 Physical aspects of the 257-260 Ma-old basalt lavas of the **Emeishan Province** of China have
 351 been studied in several sections (Huang and Opdyke, 1998; Ali et al., 2002; Liu et al., 2012; Xu et al.,
 352 2018) and modal PDFs of size distributions of the lobes consistently show them to be around 5 m for
 353 one location. Other locations have modes of ~ 12-15 m, with occasional thicker lobes up to 80 m, and
 354 even reported up to 150 m (**Figure 9A**) in others. It is not known if the thinner lobes constitute HP-
 355 type “compound” lobes or very thin SLs given the lack of relevant information in the published studies.

356 Lobe thickness data from the 251 Ma-old **Siberian Traps** are available from a cored drill hole
 357 at Norilsk (Mikhaltsov et al., 2012) and in the West Siberian Basin (Reichow et al. 2005), as well as
 358 two datasets from surface lava flow exposures in the Norilsk region (Heunemann 2003 and
 359 Krivolutskaya et al. 2018), see **Figure 9B**. The two core datasets both show a mode in the region of 5
 360 m. It is not known whether these are HP or thin SL-type lavas, but there are a few lobes reported to be
 361 in the 20 -80 m range. By contrast, the lobe thickness for the surface Norilsk lava flows is much greater
 362 with a mode from 8-20 m thickness, more analogous to other CFBs. Although each of the datasets have
 363 a few exceptionally large lobes (> 80 m thickness), we are unsure whether these measurements are
 364 accurate or are instead biased due to missing exposure.

365 There are a few measurements of lobe thicknesses from the 200-Ma-old **Central Atlantic**
 366 **Magmatic Province** (CAMP) lavas. Those from Morocco show modes of PDFs of 8-10 m (**Figure**
 367 **9C**), presumably thin SLs, with thicker lobes in places up to 50 m (Argana, El Hachimi et al., 2011;
 368 Marzoli et al., 2019). This suggests that the sequences in Morocco are dominated by thin sheet lobes,
 369 but in NE North America much thicker CAMP lobes have been recorded, with thicknesses of lobes
 370 from 60 m up to 180 m in the Newark and Fundy basins (e.g., Phillpotts et al., 1998; Whiteside, 2006;
 371 Olsen, 1980, 1989; Schaller, 2011; Puffer et al., 1992; 2018), and these are convincingly inflated SLs.

372 The **North Atlantic Magmatic Province** (NAMP) is represented by lavas from the Faroe
 373 Islands, the seafloor around that area, and a section from West Greenland. Faroes lavas were erupted
 374 subaerially around 55-57 Ma ago (Cramer et al., 2013). Basalt lava lobe thicknesses have been provided
 375 for various cored formations (Nelson, 2009; Boldreel et al., 2006; Bückner, 1998) and for exposures on
 376 the islands (Passey and Bell, 2007), see **Figure 10A**. Workers describe some formations as formed of
 377 SLs, with another of HP lavas, and another of an alternating sequence of the two: Beinisfjord Fm =
 378 SLs; Malistindar Fm = HPs; Enni Fm = alternating. Lopra borehole, which is on-land Faroes, mainly
 379 penetrated the Beinisfjord Fm (SLs); this is borne out by the data which shows lobes of mode 15 m,
 380 extending up to 60 m, like Deccan SLs. Thickness data presented for lobes in HP-dominated flows are
 381 few and ambiguous. The Enni Formation (Millet et al., 2014) shows a smaller mode than that
 382 dominated by SLs but with a tail extending to thick SL dimensions., as expected.

383 West Greenland and seafloor NAMP lavas recovered from Ocean Drilling Project cored holes
 384 (Planke, 1994) have thinner lava lobes in general (also see **Figures 10A**), the size of which overlap
 385 with the thinner lobes from the Faroes, described as “compound-braided pāhoehoe” (Passey and Bell,
 386 2007). These would be termed HP lavas by the terminology used in this study. The age and relationship
 387 of these lavas to the whole Faroes Group is not well determined.

388 Geochronology of the **Ethiopian Traps** has shown lavas about 29-30 Ma by the Ar-Ar method
 389 (Rochette et al., 1998) and lobe thicknesses are available for two sites, Belessa and Debre Sina
 390 (Lhuillier, 2018). The two sites show remarkably similar thickness variations amongst the flow lobes
 391 (**Figure 10B**), with a distinct mode in the PDF in the 8 to 10 m range, and a strong tail towards SLs as
 392 thick as 80 m. The bulk of the measurements are in the thinner range, but it is not known whether these
 393 are thin SLs or thicker HP lobes. Overall, the lobe thickness range is like that seen within the Deccan
 394 except that the main modal thickness is a little thinner than Deccan SLs and thicker than Deccan HP
 395 lobes.

396 Lobe-scale data on subaqueous LIPs are rare (Deschamps et al., 2014) but there is a little on
 397 the 125-120 Mya **Ontong Java Plateau** (Inouye et al., 2008). On Malaita Island, individual pillowed
 398 and non-pillowed basalt sheets vary in thickness between 60 cm and 80 m; about 50% of measured
 399 basalt sheets are 5–10 m thick, and >95% are less than 25 m (Petterson, 2004), similar to subaerial
 400 LIPs. Given the lack of detailed stratigraphic sections in the study, we did not plot any Ontong Java
 401 data.

402 For another comparison to CFBs, we also show data for the **Icelandic Neogene flood basalt province**
 403 which represents some of the oldest sub-aerial exposures from northwestern (~17 Ma, Riishuus et al.,
 404 2013) and northeastern Iceland (~14 Ma, Martin and Sigmarsson, 2010). Similar to other larger flood
 405 basalts, these lavas are hypothesized to be primarily erupted from dike-fed fissures and are mostly
 406 tholeiitic basalts (Walker, 1964; Gibson et al., 1966). In **Figure 10C**, we plot data from detailed
 407 stratigraphic logs from northeastern Iceland of the Kumlafell Group, Hólmatindur Group, Hjólmadalur
 408 Group, and the Grænavatn porphyritic basalt group (moving stratigraphically upward, Óskarsson &
 409 Riishuus 2014, Óskarsson et al. 2017). The mode thickness for Icelandic Neogene basalts ranges from
 410 15 m (for the first two stratigraphic groups) to 10 m (for the upper two groups). Thus, overall, the lobe
 411 thickness range is like that of Deccan SL-dominated sub-groups.

412 **Hawai’ian** lava lobe thicknesses from Kīlauea, Mauna Kea, and Mauna Loa are reported by Katz and
 413 Cashman (2003) for flows in the HSDP1 and SOH-1 cores collected on the Big Island (Garcia et al.,
 414 2007). While obviously not CFBs, these are shown here because various authors have alluded to
 415 similarities in emplacement style between Hawai’ian and CFB lava flows (e.g., Hon et al., 1994; Self
 416 et al., 1997; Sheth 2006). Kīlauean lobes are the thinnest of the Big Island volcanoes with a strong PDF
 417 mode at 3 m and a small coarser tail towards 20 m (**Figure 10D**). Mauna Loa and Mauna Kea PDFs
 418 show a broader size distribution, with stronger tails towards thicker lobes, possibly SLs, but, again,
 419 with few lobes thicker than 20 m. The modal lobe thickness is 8 m for the two large shield volcanoes,
 420 contrasting strongly with that of Kīlauea. Overall, Hawaiian SLs are thinner than in most CFB

421 provinces, and HP lobes are also thinner, especially for Kīlauea. Much more data is needed to make a
 422 definitive case for these relationships.

423 Finally, we also plot the thickness of **flow-fields**, rather than individual lobes, for a few prominent
 424 historical basaltic eruptions – the Laki 1783 eruption, the Eldgjá 934 eruption, the Holuhraun
 425 2014/2015 eruption (from Iceland), and the Kīlauea 2018 eruption (Lundgren et al., 2019, both average
 426 as well as the maximum on-land thickness near the vent). It is noteworthy that the typical flow field
 427 thicknesses for modern eruptions are like the mode of lava lobe thickness in the Deccan and CRB, as
 428 well as the Karoo, provinces. This potentially suggests that typical flow-lobe thickness for CFBs do
 429 not require extra-ordinary large eruptive fluxes *per se*, based on modern analogs. It is unclear whether
 430 the typical thickness implies a typical flow rate for all CFBs or a rheological/physical constraint on the
 431 thickness to which sheet lobes can inflate.

432 6 Discussion

433 With our full dataset, we can start comparing lobe thickness distributions for various CFBs. We note
 434 that some data sets have few measured lobes compared with others (see **Supplementary Figure 2A**
 435 **and Figure 2B**) and some warnings are given about this when the corresponding results are discussed.
 436 We display summary data on **Figure 11A** as thickness ranges per province or formation (with a range
 437 from 0-80 m), and on **Figure 11B** as “violin” plots scaled to equal width so that the total ranges can be
 438 more easily appreciated. The homogeneity of data sets from various CFB provinces is encouraging,
 439 meaning that workers in different provinces are recognizing the same features to enable them to
 440 separate the lava piles into lobes. Differences and similarities between data sets can be interpreted
 441 within currently used knowledge of lava morphology and appear to make sense. This is the first
 442 compilation of lava lobe thicknesses from CFBs and other basaltic provinces and should serve as a
 443 basic data set for future work.

444 6.1 Overall Considerations

445 The obvious difference is that non-CFB volcanoes (*sensu lato*) are generally constructed by thinner
 446 lobes than those found in most CFB provinces. Thus, Hawai’ian and the Snake River Plain basalts
 447 (Kimama borehole) lobe thicknesses stand out from CFB data on **Figures 11A and B**, having modal
 448 lobe thicknesses of 3 to 7 m. We must also remember, for CFBs, that measured thinner lobes are under-
 449 represented due to the large number of lobes involved in HP sequences. A few CFBs have equally thin
 450 lobe sets to those from non-CFB provinces, namely the Siberian core-hole for which data exists, and
 451 NAMP lavas sampled in sea-floor sequences and on West Greenland.

452 The mode of most CFB data sets ranges from 15-20 m (**Figure 11**). These are known to be SLs
 453 in the Deccan, Karoo, and CRB, and are assumed to be sheet lobes in other provinces. While very thick
 454 SLs may only occur in CFB provinces, those over 40 m thick are rare (usually outside the 75th
 455 percentile) in all provinces other than part of CAMP; for the NE North American CAMP lobes the
 456 number of measurements is small and the point about thicker lobes needs further substantiation.
 457 Overall, most CFBs have generally thicker lobes than non-CFB systems, while some CFBs have

458 equally thin lobes to non-CFB provinces. Whether this is a product of emplacement mechanism and
 459 rates, or not, awaits further data being available in the future.

460 6.2 Characteristics of Deccan Volcanic Province lavas

461 Deccan data clearly shows that lobes in the upper three formations, Mahabaleshwar, Ambenali, and
 462 Poladpur (constituting the Wai Sub-group) have thicker median and modal thicknesses than the lower
 463 formations. Cores from the Koyna area have the same range as the exposed Wai Sub-group flows
 464 which is consistent with the corresponding location of the Koyna cores in the geochemical stratigraphy
 465 Duraiswami et al., 2017). However, all formations in the cores contain lobes with smaller thicknesses,
 466 like those of the lower formations. Thick SLs (> 65 m) are outliers to the size distribution in all Wai
 467 Sub-group lavas.

468 The Lonavala Sub-group is formed by the Bushe Formation, which has a similar lobe-size
 469 distribution to the Wai lavas except for lacking lobes > ~ 20 m thick, and the Khandala Formation,
 470 which has a similar lobe-size distribution to the Wai lavas except for lacking thin lobes (but this is
 471 based on measurements in one traverse only). The lowest recognized Kalsubai Sub-group lavas range
 472 from lobes of similar thicknesses (Neral and Thakurvadi Formations) to the Wai Sub-group, to being
 473 of limited size-range (Bhimashankar Formation), but, again, data are few for the latter. Further, the
 474 whole data set under-represents the thinnest lobes, such that the modes of the Kalsubai Sub-group
 475 maybe be smaller than shown, and all Kalsubai modes are thinner than the rest of the Deccan dataset.
 476 From this we confirm past suggestions (e.g., Bondre et al., 2004) that the distribution of “compound
 477 lavas” (our thin, HP-type lobes) is due to the outcrop pattern of the stratigraphy of the Deccan and not
 478 proximity to source vents (Raja Rao et al., 1999).

479 6.3 Differences and similarities between the Deccan, CRB Province, and Karoo data sets

480 Thickness ranges for the Wanapum and Grande Ronde Formations (together forming 87 vol % of the
 481 CRB province) are similar and are also like the Wai Sub-group of the Deccan, all dominated by SLs.
 482 Still, thin lobes down to <3m thickness do exist in these CRB and Deccan formations and in the Deccan
 483 form occasional HP lava flows and/or flow-fields. Again, there is no correlation between the
 484 occurrence of HP-type lobes and proximity to source in the CRB. Data from the Karoo lavas are skewed
 485 towards thinner lobes (modes of 8-12 m) but are a mixture of HP and thin SLs according to Jay et al.
 486 (2018) and Moulin et al. (2014). These measured lavas are from one area in the Karoo Province, so
 487 may have a locational bias and not be typical of other areas of the Karoo. The relationship to source
 488 vents for the Karoo lavas is not known but Jay et al.’s (2018) work suggests the same conclusion as for
 489 the Deccan data, that HP-type lavas are not an indicator of proximity to source. In fact, the presence of
 490 flow-lobe tumuli in the Karoo lavas led Jay et al. (2018) to propose that the Naude Nek site was distal
 491 from source vents.

492 6.4 Differences and similarities with other data sets, also compared with Deccan-CRB thicknesses

493 Other thickness data sets from CFB provinces are more data-poor and perhaps less representative of
 494 the whole province. Some, e.g., the Siberian Traps borehole, must be locationally biased, having only

495 thin lobes, whereas a full range of lobe thicknesses might be expected in such a major LIP (**Figure**
496 **9B**).

497 **Figure 11B** extrapolates the lobe data ranges to include thickest outliers. It can be seen that
498 CAMP NE North America (including Fundy and North Mountain, Canada; Kontak, 2008) has the
499 thickest lobes, all nominally SLs, but this may be a reflection of the concentration of studies on thick
500 lobes which contain interesting post-emplacement features, while passing over thinner lobes? Further,
501 perhaps parts of such an old province constituted of small and thin lobes are ill-exposed or preserved,
502 as proposed for parts of the Deccan. These CAMP locations contain the thickest SLs in the whole data
503 set, with occasional lobes approaching 200 m thick in two locations (Hartford; Philpotts, 1998, and
504 Fundy; Dostal and Dupuy, 1984). It is also noteworthy that these large lobe thicknesses are comparable
505 to the large offshore thickness of Kilauea 2018 flow-field (~ 280 m). This suggests that, potentially,
506 the presence of a specific topographic break may have been responsible for the anomalously thick lobes
507 associated with CAMP. Moreover, as sills and dykes occur in the same region (Puffer et al., 1992;
508 Philpotts, 1998) these thickest lobes may have a connection with distance to source, i.e., they
509 accompany each other? This conjecture is worthy of further exploration but does not hold for the CRB
510 and Deccan province lavas.

511 In order to quantitatively compare flow-lobe thickness across various CFBs, and accounting
512 for the different flow numbers (and section thicknesses – see **Supplement Figure 2**), we use the
513 Anderson-Darling (AD) test statistic (Scholz and Stephens 1987) and the Epps-Singleton (ES) test
514 statistic (Epps & Singleton 1986) to test the likelihood that every two corresponding datasets (shown
515 in **Figure 11**) have the same underlying probability distribution (while accounting for the different
516 number of samples in the two datasets). The AD test is more sensitive towards the comparing the tails
517 of the distribution for the two datasets while the ES test is biased towards the comparing the mean
518 value of the datasets. We use the results of the pair-wise likelihood results (either ES or AD statistic)
519 for all datasets as the distance metric to perform hierarchical clustering for our lava-lobe thickness
520 dataset (Virtanen et al. 2020, Huerta-Cepas et al. 2016, **Figure 12**). These results provide a clear,
521 quantitative way to group various CFBs and nicely illustrate that the Kilauea and Kimama borehole
522 datasets are distinct from those of CFBs (**Figure 12**). Furthermore, some of the large geochemical or
523 stratigraphic units in CFBs, Grande Ronde Formation and Wai Sub-group, or Ambenali and
524 Mahabaleshwar Formations, as well as the Eastern US CAMP sections, are a distinct group. This
525 suggests some characteristic change in lava flow emplacement properties and allows a future analysis
526 of relationships between lava flow-field volumes, differences in lava geochemistry, and LIP associated
527 climatic perturbations.

528 **7 Conclusions**

529 We have summarized quantitative differences in terms of lava body thicknesses and types between the
530 main formations and sub-groups of CFB provinces, especially for the Deccan Volcanic Province. The
531 global mode for lobe thickness of pāhoehoe sheet-lobes in CFB provinces is in the range 15-20m. The
532 similarity of lobe thickness range for many CFB provinces underlines the similarity of processes on-
533 going during the emplacement of these lava flow-fields, both worldwide and throughout geologic time.

534 Furthermore, it probably also reflects the exceptionally low slopes across active LIPs. With many
 535 formations in CFB provinces displaying a range of lobe thicknesses and having hummocky-pāhoehoe-
 536 type lobes and units, it is difficult to generally accept emplacement-related criteria, e.g., closeness to
 537 vents, based on lobe characteristics.

538 For thin-lobe-dominated, or hummocky pahoehoe (HP), flow-fields, the number of thin lobes
 539 and the mean thickness will always be under-represented because they are too numerous and/or
 540 weathered to measure accurately. HP flow-fields represent approximately 5 % of the total thickness of
 541 the Deccan Wai Sub-group but up to 77 % in some formations in the Kalsubai Sub-group (the latter
 542 based on one traverse only, Jay, 2005). This estimate is biased because the older Deccan formations
 543 are under-represented in our work to date. We do note that CFBs have typically thicker flow-lobe
 544 means and modes vs Hawai'i or the Snake River Plain Province. So, on average, there may potentially
 545 be a difference in eruptive rate between these provinces. However, there is significant uncertainty from
 546 a process-scale model of what is needed to form CFB-scale inflated sheet-lobes. One can have longer-
 547 lived eruptions with 10s of km³/year magma fluxes, or 100s of km³/year fluxes of eruptions lasting for
 548 a shorter time, or something which has variations of eruptive flux between these two end-members
 549 (e.g., Laki 1783, Thordarson and Self, 2003; Rader et al., 2017). While some studies (e.g., Bondre et
 550 al., 2004) have argued for a relationship between eruption rates and flow lobe thickness, some other
 551 modern analog studies (e.g., Thordarson and Self, 1998) and experimental work (Rader et al., 2017)
 552 have not found a systematic relationship. Consequently, there is an open question whether lobe or flow
 553 thickness can be used to infer eruption rates, both absolutely (comparing, say, Hawai'i with a CFB
 554 province) or in a relative sense.

555 What gaps in knowledge exist and how this can work be applied? It is complicated to
 556 summarize single CFB province emplacement mechanisms based on good physical rationale, and
 557 single logs (small areas) can be biased and challenging from which to extrapolate. We expect some
 558 criteria expounded upon here to change, even for the Deccan, but possibly not for the Columbia River
 559 Basalt Province, with future work and data. We appeal for more data on physical lava properties from
 560 all basalt lava provinces. All data we report here are from syn- and post-Mesozoic lavas. More work is
 561 needed to compile data from pre-Mesozoic CFB province lava lobes. Some data exist but we did not
 562 expand this study to include them. Additionally, more process-based studies are required to better map
 563 the relationship between CFB lava flow morphology, particularly lobe thickness, and eruption rates.

564 **8 Conflict of Interest**

565 The authors declare that the research was conducted in the absence of any commercial or financial
 566 relationships that could be construed as a potential conflict of interest.

567 **9 Author Contributions**

568 SS is responsible for the writing, field data collection, and formulation of the study. TM is responsible
 569 for the data compilation, data analysis, as well as contribution to the writing and analysis. AJ
 570 contributed to the formulation, writing, as well as field data collection.

571 **10 Supplementary Material**

572 Supplementary Material consists of two additional figures and captions. (The Supplementary Figure
573 Captions are provided at the end of this file after main text Figure Captions.)

574 11 Data Availability Statement

575 The lava lobe thickness datasets used in this study are provided as Supplementary Files along with
576 Jupyter Notebooks for data analysis, as well as various analysis plots for each CFB dataset, at DOI:
577 10.6084/m9.figshare.13173695

578 12 Funding

579 S. Self acknowledges funding support from NSF EAR-1615021 and the Esper S. Larsen Fund of the
580 University of California, Berkeley. T. Mittal acknowledges graduate funding support from the NSF
581 grant EAR #1615203 and the Crosby Postdoc Fellowship at MIT. AEJ has been supported by The
582 Open University (UK), a NERC (UK) studentship, and the Daphne Jackson Trust.

583 13 Acknowledgments

584 We thank Mark Richards suggesting this study, and for reading and commenting upon an early version
585 of the manuscript, and Paul Renne, Benjamin Black, Michael Manga, and Loyc Vanderkluisen for
586 useful discussions. We thank Andrea Marzoli and an anonymous reviewer, and Aaron Pietruszka
587 (Special Topic editor) for their valuable comments.

588 14 Figure Captions

589 **Figure 1 (A)** Simplified geologic map of India showing distribution of main outcrops of Deccan
590 Volcanic Province (DVP) and main sub-provinces (Deccan Plateau including the Western Ghats),
591 Satpura region, Mandla Lobe, Malwa Plateau, and Kutchh-Saurashtra region (blue color). Figure also
592 shows major sedimentary basins (with Gondwana basins highlighted in red), Proterozoic mobile
593 belts, and major cratons: 1: Western Dharwar Craton, 2: Eastern Dharwar Craton, 3: Bastar Craton,
594 4: Eastern Ghats Belt, 5: Singhbhum Craton, 6: Bundelkhand Craton, 7: Aravalli Craton. Primary
595 tectonic faults and lineaments (dashed lines) in Central India related to pre-existing Indian crustal
596 features are: Barmer-Cambay rift zone, Central India Tectonic Zone (CITZ), Pranhita-Godavari rift
597 zone (PGR), Kurduwadi Lineament zone (KLZ), Western Ghats Escarpment, Koyna Fracture Zone,
598 and Ln 1-5 (lineaments inferred based on integrated analysis of gravity and magnetic data, Rajaram
599 et al., 2017). **(B)** Map of Western Ghats area where majority of DVP data comes from (Jay 2005);
600 traverses for lava data shown in blue (see **Figure 4**). **(C)** Sketch map of DVP showing Deshmukh's
601 (1988) distribution of simple and compound lavas. Mumbai is located on all three maps.

602 **Figure 2 (A)** Cartoon of section through hypothetical sheet flow lobe, after Thordarson and Self
603 (1998), showing common arrangement of internal physical features; right face: UC - upper crustal
604 zone; C - core; LC lower crustal zone; HVZ - horizontal vesicular zone; MV - megavesicles; VC -
605 vesicle cylinders; PV - pipe vesicles; BVZ - basal vesicular zone; left face shows typical form and
606 arrangement of cooling joints. On left, an ~ 1 m thick lava lobe on Kilauea, Hawai'i, formed about
607 1991, showing all features on cartoon. **(B)** Comparison of logs of poorly exposed Deccan lavas
608 where Ambenali Ghat climbs through upper part of Mahabaleshwar Fm sequence with
609 stratigraphically equivalent lavas at Arthur's Seat, 7 km to north along strike, dominated by thick
610 sheet lobes (inset photo shows the ~ 60-m-thick lobes at Window Rock, Arthur's Seat, people for
611 scale!). Ambenali Ghat road area is thought to have poor exposure due to presence of thinner lobes
612 that are more prone to erosion and weathering, representing lateral transition from thick sheet-lobe-
613 dominated cliff exposures to N (Arthur's Seat) to an area dominated by thinner lobes; modified from

614 Jay (2005). **(C)** Cartoon of hummocky pāhoehoe pile of lava forming through stages A-C, based on
 615 lavas in the Kimama drill core, Snake River Plain, after Potter et al., (2019).

616 **Figure 3 (A)** Detailed log of small section of Ambenali Ghat traverse, Deccan Volcanic Province,
 617 within Ambenali Formation lavas (see 3B) illustrating variety of morphologies in lava flows within
 618 one chemo-stratigraphic formation. Section is from 550-680 m above sea level and shows several
 619 sheet lobes under- and overlain by smaller precursor and break-out lobes, respectively, as well as
 620 other physical lava features indicated on key: from Jay (2005). **(B)** Composite section of Western
 621 Ghats lava flow stratigraphy showing geochemically defined formations (following Beane et
 622 al.,1986). This study includes data from all named formations except Jawar, Igatpuri, and Panhala.
 623 Magnetic polarity of lavas is expressed at right, R – chron 29r; N = chron 29n, after Jay et al., (2009).
 624 **(C)** Simplified stratigraphic logs of various Deccan transects showing geochemical formations
 625 (following Jay et al., 2009).

626 **Figure 4 (A)** Plots of lobe thickness in each Deccan lava formation vs altitude above mean sea level
 627 for traverses in central Western Ghats area; width of bar = lobe thickness (see **Figure 1B** for traverse
 628 locations). Formations are shown by bar color (see key); + open dots = with small lobes; + stars =
 629 small-lobe-dominated. Red vertical lines show boles (weathering horizons, see text, note the bole line
 630 thickness is not to scale). Note also that lobes > 40 m thick are uncommon. **(B)** Flow thickness
 631 plotted against elevation above mean sea level in six logs through parts of Western Ghats lava series.
 632 Plots given from N to S (top to bottom; see Figure 1B for traverse locations) represent distance of ~
 633 80 km. Formation ornaments as on **(A)**.

634 **Figure 5 (A)** Plots of univariate kernel density estimators to calculate probability density function
 635 (PDF) of lava lobe thicknesses in DVP data set. Vertical scale is % of PDF with area under PDF
 636 curve normalizing to one. Result for each recognized formation is arranged from youngest to oldest
 637 (top to bottom) with ticks at base of each plot showing actual value of measured lava lobe
 638 thicknesses. **(B)** Univariate kernel density estimator to calculate probability density function (PDF)
 639 of lava lobe thicknesses in accumulated formations within each Deccan subgroup, see **Figure 3B**.
 640 Plot gives useful view of whole thickness distribution at a glance: middle (Lonavala) subgroup has
 641 one modal lobe thickness of ~ 18 m and another at ~ 50 m; lowest (Kalsubai) subgroup has smallest
 642 modal lobe thickness and coarse tail extending towards 50 m; upper (Wai) subgroup has same
 643 median thickness as middle subgroup and coarse tail extending towards 100 m. Each subgroup has
 644 small lobes and lowest one contains highest percentage.

645 **Figure 6 (A)** Violin plot of flow lobe thickness variation (y axis) vs formations in various traverses
 646 through DVP lavas of Western Ghats (x axis). Width of violin represents amount of data for each
 647 formation and thickness range encapsulated in vertical distribution. White dot marks mean of
 648 distribution and black bar 75th – 25th percentile range. **(B)** Same as **5B**, but with PDF for two Koyna
 649 area cores added (Koyna); note similarity with upper (Wai) sub-group PDF. In addition, flow lobe
 650 thickness datasets shown for Killari region (South-Eastern Deccan Plateau, Wai subgroup flows), and
 651 Deccan sub-Provinces (Mandla, Malwa, Narmada-Tapi Rift Zone = Satpura, and North Western
 652 Deccan = Cambay Rift Zone/Saurashtra, see **Figure 1A**).

653 **Figure 7 (A)** Plots of lobe thickness for Lesotho part of Karoo CFB Province from Jay et al., (2018)
 654 and Moulin et al., (2017) plotted as function of altitude above mean sea level; width of bar = lobe
 655 thickness. Groups shown by bar color (see key in **B**); + open dots = with small lobes; + stars = small-
 656 lobe-dominated. Red vertical lines = boles (weathering horizons, note bole line thickness not to
 657 scale). **(B)** Plots of univariate kernel density estimators to calculate PDFs of lava lobe thicknesses of

658 three Karoo sequences. Note relative similarity of the three distributions, due to SLs from 15- 18 m
 659 thick, with Naude Nek lobes being a little thinner due to prevalence of HP lobes down to a few
 660 meters thickness.

661 **Figure 8 (A)** Plots of univariate kernel density estimators to calculate PDF of lava lobe thicknesses
 662 for individual Wanapum Formation eruptive flow-fields (Palouse Falls; Gingko; Sand Hollow;
 663 Roza), Wanapum Formation data collectively, and Grande Ronde and Wallula Grand Ronde
 664 Formations; both the latter plots are Grande Ronde Basalt Formation (see text) from the Columbia
 665 River Basalt Province. **(B)** Summary PDFs of lava lobe thicknesses for individual Wanapum eruptive
 666 flow-fields (Palouse Falls; Gingko; Sand Hollow; Roza), Wanapum Formation data collectively, and
 667 Grande Ronde and Wallula Grand Ronde plots, which are Grande Ronde Basalt Formation (see text).
 668 **(B, inset)** shows plot of univariate kernel density estimators to calculate PDF of lobe thicknesses for
 669 lavas of Kimama Borehole, Snake River Plain (after Potter et al., 2019); note thinness *cf.* Columbia
 670 River Basalt data.

671 **Figure 9 (A)** Plot of univariate kernel density estimators to calculate PDFs of lobe thicknesses for
 672 lavas of CAMP Province in Morocco (including Argana Basin) and NE North America (Newark and
 673 Fundy Basins). **(B)** Plot of univariate kernel density estimators to calculate PDF of lobe thicknesses
 674 for lavas from Siberian CFB Province, Russia; see text for details. **(C)** Plot of univariate kernel
 675 density estimators to calculate PDF of lobe thicknesses for lavas of Emeishan CFB Province, China,
 676 from 4 different areas; see text for details.

677 **Figure 10 (A)** Plot of univariate kernel density estimators to calculate PDF of lobe thicknesses for
 678 NAIP formations in Faroe Islands, West Greenland, and the North Sea floor (ODP data); see text for
 679 details. **(B)** Plot of univariate kernel density estimators to calculate PDF of lobe thicknesses for lavas
 680 from Ethiopian Traps; see text for details. **(C)** Plot of univariate kernel density estimators to calculate
 681 PDF of lobe thicknesses for lavas from the Neogene Flood Basalt Province in Iceland along with
 682 typical flow lobe thickness for a few modern eruptions. See text for details. **(D)** Plot of univariate
 683 kernel density estimators to calculate PDF of lobe thicknesses for lavas from island of Hawa'i,
 684 including Mauna Loa, Mauna Kea, and Kīlauea. See text for details.

685 **Figure 11 (A)** Box plot of lobe thicknesses in various CFB provinces, formations, and volcanoes for
 686 which data is available vs thickness of lobes. CFB provinces color-coded so that formations of each
 687 province have same color (and same colors as **Figure 12**). Bar in box is median (50th percentile);
 688 ends of box are 25th and 75th percentile; whisker ends are 5th and 95th percentile, and dots are
 689 outlying thicknesses of whole lobe thickness distribution for each entry. Data cut off at 75 m
 690 thickness; see (B) for whole range. **(B)** Violin plot of lobe thicknesses in various CFB provinces,
 691 formations, and volcanoes for which data is available vs thickness of lobes. Violins scaled to equal
 692 width so that total ranges more easily seen; as (A) for colors. White dot inside violin is median (50th
 693 percentile); ends of box are 25th and 75th percentile; line ends are 5th and 95th percentile; rest of
 694 violin encloses all data of whole lobe thickness distribution for each entry.

695 **Figure 12 (A)** Clustering of flow lobe thickness distributions using distance metric based on
 696 Anderson-Darling statistical tests. CFB provinces are color-coded so that formations of a CFB
 697 Province have the same color (same colors as **Figure 11**). CFB Provinces are clustered into 3 distinct
 698 sub-groups highlighting classes of PDFs. **(B)** Clustering of flow lobe thickness distributions using
 699 distance metric based on Epps Singleton statistical tests. CFB provinces are color-coded so that
 700 formations of a CFB province have the same color (same colors as **Figure 11**). CFB provinces are
 701 clustered into 3 distinct sub-groups highlighting classes of PDFs.

702 **Figure Captions – Supplementary Figures**

703 **Figure SM1** Excerpts from lithostratigraphic logs (Jay, 2005) showing features of lavas in selected
 704 parts of seven traverses representing typical features of DVP lava formations. Key gives
 705 identification of lava features, together with paleomagnetic polarity signature and
 706 formation/chemotype [see Jay et al., 2009]; m asl - height above sea level. No correlations between
 707 lavas are indicated by placement of logs in this figure. Logs except Matheran show types of sheet
 708 lobes and hummocky-pāhoehoe plotted in **Figure 4**.

709 **Figure SM2** Summary statistics of total flow lobe thickness dataset. In Panel **A**, total combined
 710 section thickness for various CFB provinces is shown while Panel **B** shows total number of flows
 711 corresponding to various subgroups/formations/locations for these provinces.

712 **15. References:**

- 713 Ali, J.R., Thompson, G.M., Song, X., and Wang, Y. (2002). Emeishan Basalts (SW China) and the
 714 'end-Guadalupian' crisis: magnetobiostratigraphic constraints. *J. Geol. Soc.* 159(1), 21-29.
- 715 Barry, T.L., Self, S., Kelley, S.P., Reidel, S., Hooper, P., and Widdowson, M. (2010). New $^{40}\text{Ar}/^{39}\text{Ar}$
 716 dating of the Grande Ronde lavas, Columbia River Basalts, USA: Implications for duration of flood
 717 basalt eruption episodes. *Lithos* 118, 213–222. doi.org/10.1016/j.lithos.2010.03.014
- 718 Beane, J.E., Turner, C.A., Hooper, P.R., Subbarao, K.V. and Walsh, J.N. (1986). Stratigraphy,
 719 composition and form of the Deccan Basalts, Western Ghats, India. *Bull. Volcanol.* 48, 61-83.
- 720 Boldreel, L.O. (2006). Wire-line log-based stratigraphy of flood basalts from the Lopra-1/1A well,
 721 Faroe Islands. *Geol. Surv. Denmark and Greenland (GEUS) Bull.* 9, 7-22.
- 722 Bondre, N.R., Duraiswami, R.A., and Dole, G. (2004). Morphology and emplacement of flows from
 723 the Deccan Volcanic Province. *Bull. Volcanol.* 66, 29–45.
- 724 Brown, R.J., Blake, S., Bondre, N.R., Phadnis, V.M., and Self, S. (2011) 'A'ā lavas in the Deccan
 725 Volcanic Province, India, and their significance to the nature of continental flood basalt eruptions.
 726 *Bull. Volcanol.* 73, 737-752.
- 727 Bücker, C.J., Delius, H., and Wohlenberg, J. (1998). Physical signature of basaltic volcanics drilled
 728 on the northeast Atlantic volcanic rifted margins. *Geol. Soc., London, Special Pubs.* 136(1), 363-374.
- 729 Chenet, A.L., Fluteau, F., Courtillot, V., Gerard, M., and Subbarao, K.V. 2008. Determination of
 730 rapid eruption across the Cretaceous–Tertiary boundary using paleomagnetic secular variation:
 731 Results from a 1200 m thick section in the Mahabaleshwar Escarpment. *J. Geophys. Res.* 113, 27 p.
 732 doi:10.1029/2006JB004635.
- 733 Clapham, M.E., and Renne, P.R. (2019). Flood basalts and mass extinctions. *Ann. Rev. Earth Planet.*
 734 *Sci.* 47, 275-303.
- 735 Cramer E.L., Sherlock S.C., Halton A.M., and Blake, S. (2013). Which age is the true age?
 736 Unravelling within-flow $^{40}\text{Ar}/^{39}\text{Ar}$ age variations in Faroe Islands basalt lavas. Conference paper:
 737 *Goldschmidt Volume: Min. Mag.* 77, 924.

- 738 Deschamps, A., Grigné, C., Le Saout, M., Soule, S.A., Allemand, P., Van Vliet-Lanoe, B., and
 739 Floc'h, F. (2014). Morphology and dynamics of inflated subaqueous basaltic lava flows. *Geochem.,*
 740 *Geophys., Geosystems* 15(6), 2128-2150.
- 741 Deshmukh, S.S. (1988). "Petrographic variations in compound flows of Deccan Traps and their
 742 significance", in *Deccan Flood Basalts, Geol. Soc. India Memoir* 10, ed K.V. Subbarao (Bangalore,
 743 Geological Society of India), 305 – 319.
- 744 Doke, S.B. (2014). Unpublished PhD Thesis, Study of Deccan Trap Flows In Chikhaldara Ghat
 745 Section, District of Amravati. Dr. Babasaheb Ambedkar Marathwada University, 2014.
- 746 Dostal, J, and Dupuy, S. (1984). Geochemistry of the North Mountain basalts (Nova Scotia, Canada).
 747 *Chem. Geol.* 45, 245-261.
- 748 Duraiswami, R.A., Gadpallu, P., Shaikh, T.N., and Cardin, N. (2014) Pahoe-hoe - a'a transitions in
 749 the lava flow fields of the western Deccan Traps, India – implications for emplacement dynamics,
 750 flood basalt architecture and volcanic stratigraphy. *J. Asian Earth Sci.* 84, 146 – 166.
- 751 Duraiswami, R.A., Gadpallu, P., Maskare, B., Purwant, A., Meena, P., Krishnamurthy, P., and
 752 Mahabaleshwar, B. (2017). Volcanology and lava flow morpho-types from the Koyna-Warna,
 753 Region, Western Deccan Traps, India. *J. Geol. Soc. India* 90, 742-747
- 754 El Hachimi, H., Youbi, N., Madeira, J., and 11 others (2011). Morphology, internal architecture and
 755 emplacement of lava flows from the Central Atlantic Magmatic Province (CAMP) of Argana Basin
 756 (Morocco). *Geol. Soc. London, Spec. Pubs.* 357, 167-193. doi: 10.1144/SP357.9
- 757 Epps, W., and Singleton, K.J. (1986). An omnibus test for the two-sample problem using the
 758 empirical characteristic function. *J. Statist. Comp. Simul.* 26, 177–203.
- 759 Ernst, R.E., Liikane, D.A., Jowitt, S.M., Buchan, K.L., and Blanchard, J.A. (2019). A new plumbing
 760 system framework for mantle plume-related continental Large Igneous Provinces and their mafic-
 761 ultramafic intrusions. *J. Volc. Geotherm. Res.* 384, 75-84.
- 762 Garcia, M.O., Haskins, E.H., Stolper, E.M., and Baker, M. (2007). Stratigraphy of the Hawai'i
 763 Scientific Drilling Project core (HSDP2): Anatomy of a Hawai'ian shield volcano. *Geochem.,*
 764 *Geophys., Geosystems* 8(2). 2006GC001379. ISSN 1525-2027.
- 765 Gibson, I.L. (1966). The crustal structure of eastern Iceland. *Geophys. J. Internat.* 12(1), 99-102.
- 766 Godbole, S.M., Rana, R.S. and Natu, S.R. (1996) "Lava Stratigraphy of Deccan Basalts of Western
 767 Maharashtra", in *Deccan Basalts, Spec. Pub. Gondwana Geol. Soc.* 2, eds S.S. Deshmukh and
 768 K.K.K. Nair (Bombay: Gondwana Geol. Soc.), 125-134.
- 769 Greeley, R. (1982) The Snake River Plain, Idaho: Representative of a new category of volcanism. *J.*
 770 *Geophys Res.* 87 B4, 2705–2712.
- 771 Gupta, H.K., Srinivasan, R., Rao, R.U.M., Rao, G.V., Reddy, G.K., Roy, S., and Parthasarathy, G.
 772 (2003). Borehole investigations in the surface rupture zone of the 1993 Latur SCR earthquake,
 773 Maharashtra, India: overview of results. *Geol. Soc. India Mems*, 1-22.

- 774 Guilbaud, M. N., Self, S., Thordarson, T., & Blake, S. (2005). Morphology, surface structures, and
 775 emplacement of lavas produced by Laki, AD 1783–1784. *Geological Society of America Special
 776 Papers*, 396, 81-102.
- 777 Hon, K., Kauahikaua, J., Denlinger, R., and Mackay, K. (1994). Emplacement and inflation of
 778 pahoehoe sheet flows: observations and measurements of active lava flows on Kilauea Volcano,
 779 Hawai'i. *Geol. Soc. Amer., Bull.* 106, 351 - 370.
- 780 Heunemann, C. (2003). Direction and Intensity of Earth's Magnetic Field at the Permo-Triassic
 781 Boundary: A Geomagnetic Reversal Recorded by the Siberian Trap Basalts, Russia (Doctoral
 782 dissertation, Verlag nicht ermittelbar).
- 783 Huang, K., and Opdyke, N.D. (1998). Magnetostratigraphic investigations on an Emeishan basalt
 784 section in western Guizhou province, China. *Earth Planet. Sci. Lett.* 163(1-4), 1-14.
- 785 Huerta-Cepas, J., Serra, F., and Bork, P. (2016). ETE 3: Reconstruction, analysis and visualization of
 786 phylogenomic data. *Molec. Biol. Evol.*; doi: 10.1093/molbev/msw046
- 787 Hull, P.M., Bornemann, A., Penman, D.E., Henahan, M.J., Norris, R.D., Wilson, P.A., Blum, P., et
 788 al. (2020). On impact and volcanism across the Cretaceous-Paleogene boundary. *Science* 367, no.
 789 6475, 266-272.
- 790 Inoue, H., Coffin, M.F., Nakamura, Y., Mochizuki, K., and Kroenke, L.W. (2008). Intrabasement
 791 reflections of the Ontong Java Plateau: Implications for plateau construction. *Geochem. Geophys.
 792 Geosystems* 9.4. <https://doi.org/10.1029/2007GC001780>.
- 793 Jay, A.E. (2005). Volcanic architecture of the Deccan Traps, Western Maharashtra, India: an
 794 integrated chemostratigraphic and palaeomagnetic study. PhD thesis, Open University, Milton
 795 Keynes.
- 796 Jay, A.E., Marsh, J.S., Fluteau, F., and Courtillot, V.E. (2018). Inflated pāhoehoe flows in the
 797 Naude's Nek Pass, Lesotho remnant, Karoo continental flood basalt Province: use of flow-lobe
 798 tumuli in understanding flood basalt emplacement. *Bull. Volcanol.* 80, 17. doi.org/10.1007/s00445-
 799 017-1189-6
- 800 Jay, A.E., MacNiocall, C., Self, S., Widdowson, M., and Turner, W. (2009). New paleomagnetic data
 801 from the Mahabaleshwar plateau, Deccan Province: Implications for volcanostratigraphic architecture
 802 of continental flood basalt Provinces. *J. Geol. Soc. London* 166, 13-24.
- 803 Jay, A.E., and Widdowson, M. (2008). Stratigraphy, structure and volcanology of the SE Deccan
 804 continental flood basalt Province: implications for eruptive extent and volumes. *J. Geol. Soc. London*
 805 165, 177–188. doi.org/10.1144/0016-76492006-062
- 806 Kale, V.S., Bodas, M., Chatterjee, P., and Pande, K. (2020a). Emplacement history and evolution of
 807 the Deccan Volcanic Province, India. *Episodes* 43.1, Special Issue: *Geodynamic evolution of the
 808 Indian subcontinent*, 278-298.
- 809 Kale, V.S., Dole, G., Shandilya, P., and Pande, K. (2020b). Stratigraphy and correlations in Deccan
 810 Volcanic Province, India: quo vadis? *Geol. Soc. Amer. Bull.* 132(3-4), 588-607.

- 811 Kasbohm, J., and Schoene, B. (2018). Rapid eruption of the Columbia River flood basalt and
812 correlation with the mid-Miocene climate optimum. *Science Adv.* 4: eaat8223, 9 p.
- 813 Kasiviswanandham, A. (2003). Flow Stratigraphy and Paleomagnetic Investigations of Bagli
814 Volcanics, Malwa Deccan Traps MP, and To Develop Constraints on its Petrogenesis. Sant Gadge
815 Baba Amravati University, <http://hdl.handle.net/10603/147752>
- 816 Katz, M.G., and Cashman, K.V. (2003). Hawai'ian lava flows in the third dimension: Identification
817 and interpretation of pahoehoe and 'a'a distribution in the KP-1 and SOH-4 cores. *Geochem.,*
818 *Geophys., Geosystems* 4, 1–24. doi: 10.1029/2001GC000209
- 819 Kilburn, C.R.J., and Lopes, R.C.M. (1991). General patterns of flow field growth: aa and blocky
820 lavas. *J. Geophys. Res.* 96, 19,721-19,732.
- 821 Kontak, D.J. (2008). On the edge of CAMP: Geology and volcanology of the Jurassic North
822 Mountain Basalt, Nova Scotia. *Lithos* 101, 74-101.
- 823 Krivolutsкая, N.A., Kuzmin, D.V., Gongalsky, B.I., Roshchina, I.A., Kononkova, NN., Svirskaya,
824 N. M., and Romashova, T.V. (2018). Stages of trap magmatism in the Norilsk area: New data on the
825 structure and geochemistry of the volcanic rocks. *Geochem. Internat.* 56(5), 419-437.
- 826 Kumar, K.V., Chavan, C., Sawant, S., Raju, K.N., Kanakdande, P., Patode, S., and Balaram, V.
827 (2010). Geochemical investigation of a semi-continuous extrusive basaltic section from the Deccan
828 Volcanic Province, India: implications for the mantle and magma chamber processes. *Contrib.*
829 *Mineral. Petrol.* 159(6), 839-862.
- 830 Landwehrs, J.P., Feulner, G., Hofmann, M., and Petri, S. (2020). Climatic fluctuations modeled for
831 carbon and sulfur emissions from end-Triassic volcanism. *Earth Planet. Sci. Lett.* 537, 116174.
- 832 Lhuillier, F., and Gilder, S.A. (2019). Palaeomagnetism and geochronology of Oligocene and
833 Miocene volcanic sections from Ethiopia: geomagnetic variability in the Afro-Arabian region over
834 the past 30 Ma. *Geophys. J. Internat.* 216.2, 1466-1481.
- 835 Liu, C., Pan, Y., and Zhu, R. (2012). New paleomagnetic investigations of the Emeishan basalts in
836 NE Yunnan, southwestern China: Constraints on eruption history. *J. Asian Earth Sci.* 52, 88-97.
- 837 Lundgren, P.R., Bagnardi, M., and Dietterich, H. (2019). Topographic Changes During the 2018
838 Kīlauea Eruption from Single-pass Airborne InSAR. *Geophys. Res. Lett.* 46, 9554–9562.
839 <https://doi.org/10.1029/2019GL08350>
- 840 Mahoney, J.J., Macdougall, J.D., Lugmair, J.W., Murali, A.V., Sankar Das, M., and Gopalan, K.
841 (1982). Origin of the Deccan Trap flows at Mahabaleshwar inferred from Nd and Sr isotopic and
842 chemical evidence. *Earth Planet. Sci. Lett.* 60, 47-60.
- 843 Mahoney, J.J., Sheth, H.C., Chandrasekharam, D., and Peng, Z.X. (2000). Geochemistry of flood
844 basalts of the Toranmal section, northern Deccan Traps, India: implications for regional Deccan
845 stratigraphy. *J. Petrol.* 41(7), 1099-1120.
- 846 Martin, E., and Sigmarsson, O. (2010). Thirteen million years of silicic magma production in Iceland:
847 Links between petrogenesis and tectonic settings. *Lithos* 116(1-2), 129-144.

- 848 Marzoli, A., Bertrand, H., Youbi, N., and 18 others (2019). The Central Atlantic Magmatic Province
849 (CAMP) in Morocco. *J. Petrol.* 2019, 1–51. doi: 10.1093/petrology/egz021
- 850 Mikhailtsov, N.E., Kazansky, A.Y., Ryabov, V.V., Shevko, A.Y., Kuprish, O. V., and Bragin, V.Y.
851 (2012). Paleomagnetism of trap basalts in the northwestern Siberian craton, from core data. *Russian*
852 *Geol. Geophys.* 53(11), 1228-1242.
- 853 Millett, J.M., Hole, M.J., Jolley, D.W., and Passey, S.R. (2017). Geochemical stratigraphy and
854 correlation within large igneous provinces: the final preserved stages of the Faroe Islands Basalt
855 Group. *Lithos* 286, 1-15.
- 856 Mishra, S., Misra, S., Vyas, D., Nikalje, D., Warhade, A and Roy, S. (2017) A 1251 m thick Deccan
857 flood basalt pile recovered by scientific drilling in the Koyna region, Western Maharashtra. *J. Geol.*
858 *Soc. India* 90, 788 – 794.
- 859 Mitchell, C., and Widdowson, M. (1991). A geological map of the southern Deccan Traps, India and
860 its structural implications. *J. Geol. Soc. London* 148, 495–505.
- 861 Moulin, M., Fluteau, F., Courtillot, V.E., et al., (2017). Eruptive history of the Karoo lava flows and
862 their impact on early Jurassic environmental change. *J. Geophys. Res., Solid Earth* 122, 738–772.
863 doi.org/10.1002/2016JB013354
- 864 Nelson, C.E., Jerram, D.A., and Hobbs, R.W. (2009). Flood basalt facies from borehole data:
865 implications for prospectivity and volcanology in volcanic rifted margins. *Petroleum Geosci.* 15(4),
866 313-324.
- 867 Olsen, P.E. (1980). “Triassic and Jurassic formations of the Newark Basin”, in *Field studies of New*
868 *Jersey geology and guide to field trips: 52nd annual meeting of the New York State Geological*
869 *Association*, ed. W. Manspeizer (pp. 2-41).
- 870 Olsen, P.E., Schlische, R.W., Gore, P.J.W., eds. (1989). “Field Guide to the Tectonics, Stratigraphy,
871 Sedimentology, and Paleontology of the Newark Supergroup, Eastern North America.” *Internat.*
872 *Geol. Congress, Guidebooks for Field Trips*, vol. T351: 174 pp.
- 873 Óskarsson, B.V., and Riishuus, M.S. (2014). The mode of emplacement of Neogene flood basalts in
874 eastern Iceland: Facies architecture and structure of simple aphyric basalt groups. *J. Volc. Geotherm.*
875 *Res.* 289, 170-192.
- 876 Óskarsson, B.V., Andersen, C.B., Riishuus, M.S., Sørensen, E.V., and Tegner, C. (2017). The mode
877 of emplacement of Neogene flood basalts in Eastern Iceland: The plagioclase ultraphyric basalts in
878 the Grænavatn group. *J. Volc. Geotherm. Res.* 332, 26-50.
- 879 Passey S.R., and Bell, B.R. (2007). Morphologies and emplacement mechanisms of the lava flows of
880 the Faroe Islands Basalt Group, Faroe Islands, NE Atlantic Ocean. *Bull. Volcanol.* 70, 139-156.
- 881 Pathak, V., Patil, S.K., and Shrivastava, J.P. (2017). Tectonomagmatic setting of lava packages in the
882 Mandla lobe of the eastern Deccan volcanic province, India: palaeomagnetism and
883 magnetostratigraphic evidence. *Geol. Soc., London, Spec. Pubs.* 445(1), 69-94.

- 884 Peng, Z.X., and Mahoney, J.J. (1995). Drillhole lavas from the northwestern Deccan Traps, and the
885 evolution of Réunion hotspot mantle. *Earth Planet. Sci. Lett.* 134(1-2), 169-185.
- 886 Petterson, M.G. (2004). The geology of north and central Malaita, Solomon Islands: The thickest and
887 most accessible part of the world's largest (Ontong Java) ocean plateau. *Geol. Soc., London, Spec.*
888 *Pubs.* 229.1, 63-81.
- 889 Philpotts, A.R. (1998). Nature of a flood-basalt-magma reservoir based on the compositional
890 variation in a single flood-basalt flow and its feeder dike in the Mesozoic Hartford Basin,
891 Connecticut. *Contrib. Mineral. Petrol.* 133, p. 69–82. doi.org/10.1007/s004100050438.
- 892 Planke, S. (1994). Geophysical response of flood basalts from analysis of wire line logs: Ocean
893 Drilling Program Site 642, Vøring volcanic margin. *J. Geophys. Res., Solid Earth* 99(B5), 9279-
894 9296.
- 895 Potter, K.E., Champion, D.E., Duncan, R.A., and Shervais, J.W. (2019). Volcanic stratigraphy and
896 age model of the Kimama deep borehole (Project Hotspot): Evidence for 5.8 million years of
897 continuous basalt volcanism, central Snake River Plain, Idaho. *Geosphere* 15,
898 doi.org/10.1130/GES01679.1.
- 899 Puffer, J.H., Block, K.A., Steiner, J.C., and Laskowich, C. (2018). Complex layering of the Orange
900 Mountain Basalt: New Jersey, USA. *Bull. Volcanol.* 80: 54. (<https://doi.org/10.1007/s00445-018-1231-3>).
- 902 Puffer, J.H., Husch, J.M., and Benimoff, A.I. (1992). The Palisades Sill and Watchung Basalt Flows,
903 Northern New Jersey and Southeastern New York: A Geological Summary and Field Guide. *New*
904 *Jersey Geological Survey Open-File Report OFR 92-1*.
- 905 Rader, E., Vanderkluysen, L., and Clarke, A.B. (2017). The role of unsteady effusion rates on
906 inflation in long-lived lava flow fields. *Earth Planet. Sci. Lett.* 477, 73-83.
- 907 Rajaram, M., Anand, S.P., Erram, B.N. and Shinde, B.N. (2017).” Insight into the structures below
908 the Deccan Trap-covered region of Maharashtra, India, from geopotential data”, in Mukherjee, S.,
909 Misra, A.A., Calve's, G., and Nemečok, M. (eds) *Tectonics of the Deccan Large Igneous Province*.
910 Geological Society, London, Special Publications 445, 219–236. , <https://doi.org/10.1144/SP445.8>
- 911 Raja Rao, C.S., Sahasrabudhe, Y.S., Deshmukh, S.S., and Raman, R. (1999). "Distribution, Structure
912 and Petrography of the Deccan Traps, India, in *Deccan Volcanic Province*. *Geol. Soc. India Memoir*
913 *43-1*, ed K.V. Subbarao. Bangalore, *Geol. Soc. India*, p. 401-414.
- 914 Reichow, M.K., Saunders, A.D., White, R.V., Al'Mukhamedov, A.I., and Medvedev, A.Y. (2005).
915 Geochemistry and petrogenesis of basalts from the West Siberian Basin: an extension of the Permo–
916 Triassic Siberian Traps, Russia. *Lithos*, 79(3-4), 425-452.
- 917 Renne, P.R., Sprain, C.J., Richards, M.A., Self, S., Vanderkluysen, L., and Pande, K. (2015). State
918 shift in Deccan volcanism at the Cretaceous-Paleogene boundary, possibly induced by impact.
919 *Science* 350(6256), 76-78.

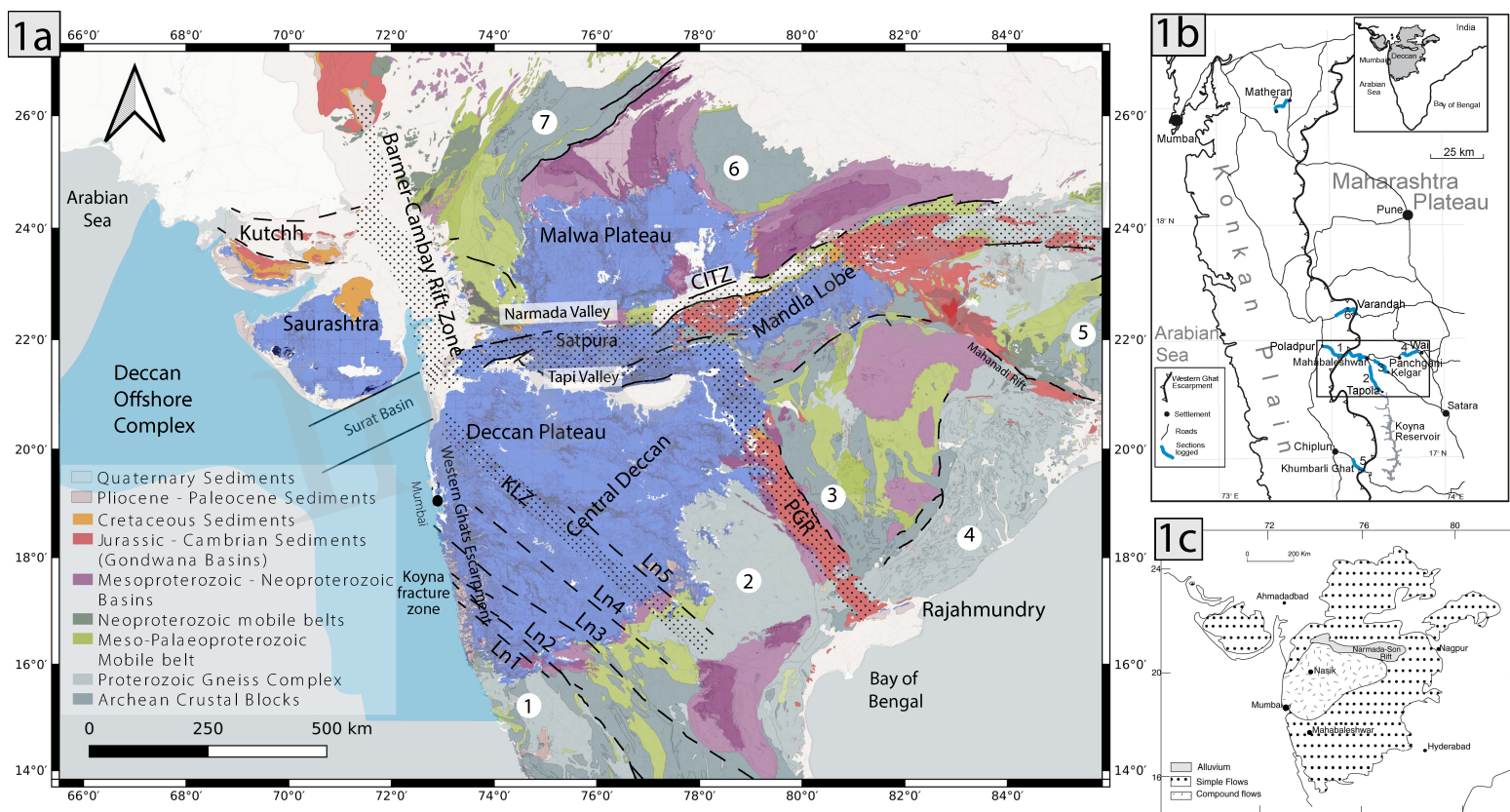
- 920 Rochette, P., Tamrat, E., Ferraud, G., Pik, R., Courtillot, V., Ketefo, E., Coulon, C., Hoffmann, C.,
 921 Vandamme, D., and Yirgu, D. (1998). Magnetostratigraphy and timing of the Oligocene Ethiopian
 922 traps. *Earth Planet. Sci. Lett.* 164, 497-510.
- 923 Schaller, M.F., Wright J.D., and Kent, D.V. (2011). Atmospheric pCO₂ perturbations associated with
 924 the Central Atlantic magmatic province. *Science* 331.602, 1404-1409.
- 925 Schmidt, A., Skeffington, R.A., Thordarson, T., Self, S., Forster, P.M., Rap, A., Ridgwell, A.,
 926 Fowler, D., Wilson, M., Mann, G.W., Wignall, P.B., and Carslaw, K.S. (2016). Selective
 927 environmental stress from sulphur emitted by continental flood basalt eruptions. *Nat. Geosci.* 9, 77–
 928 82. doi.org/10.1038/ngeo2588.
- 929 Schoene, B., Eddy, M.P., Samperton, K.M., Keller, C.B., Keller, G., Adatte, T., and Khadri, S.F.R.
 930 (2019). U-Pb constraints on pulsed eruption of the Deccan Traps across the end-Cretaceous mass
 931 extinction. *Science* 363, 862–866. doi.org/10.1126/science.aau2422.
- 932 Scholz, F.W., and Stephens, M.A. (1987). K-Sample Anderson-Darling Tests, *J. Amer. Statistical*
 933 *Assoc.* 82, 918-924.
- 934 Self, S., Thordarson, Th., and Keszthelyi, L. (1997). "Emplacement of Continental Flood Basalt Lava
 935 Flows", in *AGU Geophys. Monograph* 100, *Large Igneous Provinces*, eds J.J. Mahoney and M.F.
 936 Coffin, 381-410.
- 937 Self, S., Keszthelyi, L.P., and Thordarson, Th. (1998) The importance of pāhoehoe. *Ann. Rev. Earth*
 938 *Planet. Sci.* 26, 81–110.
- 939 Self, S., Jay, A.E., Widdowson, M., and Keszthelyi, L.P. (2008). Correlation of the Deccan and
 940 Rajamundry Trap lavas: are these the longest and largest lava flows on Earth? *J. Volcanol. Geotherm.*
 941 *Res. [Special Issue on Large Igneous Provinces]* 172, 2-19.
- 942 Self, S., Schmidt, A., and Mather, T.A. (2014). Emplacement characteristics, time scales, and
 943 volcanic gas release rates of continental flood basalt eruptions on Earth. *Geol. Soc. Am. Spec. Pap.*
 944 505. doi.org/10.1130/2014.2505(16).
- 945 Self, S., Widdowson, M., Thordarson, T., and Jay, A.E. (2006). Volatile fluxes during flood basalt
 946 eruptions and potential effects on the global environment: A Deccan perspective. *Earth Planet. Sci.*
 947 *Lett.* 248, 517–531. doi.org/10.1016/j.epsl.2006.05.041.
- 948 Sengupta, P., and Ray, A. (2006). Primary volcanic structures from a type section of Deccan Trap
 949 flows around Narsingpur-Harrai-Amarwara, central India: Implications for cooling history. *J. Earth*
 950 *System Sci.* 115(6), 631-642.
- 951 Sharma, K., Keszthelyi, L., Thornber, C., and Self, S. (2000). Variations in Cooling, Crystallization
 952 Textures, and Glass Chemistry During Emplacement of Kilauea Pahoehoe Lobes, as Constrained by
 953 In Situ Field Experiments. *GSA Abstracts with Programs* 32, no. 7.
- 954 Sheth, H.C. (2006). The emplacement of pahoehoe lavas on Kilauea and in the Deccan traps. *J. Earth*
 955 *Syst. Sci.* 115, 615-629.

- 956 Sheth, H.C., and Cañón-Tapia, E. (2015). Are flood basalt eruptions monogenetic or polygenetic?
957 *Internat. J. Earth Sci.* 104(8), 2147-2162.
- 958 Sinha, D.K., Som, A., and Roy, S. (2017) The subsurface megascopic characteristics of basalt and
959 basement rocks from Koyna-Warna area of Maharashtra, India. *J. Geol. Soc. India* 90, 761–768.
- 960 Sprain, C.J., Renne, P.R., Vanderkluysen, L., Pande, K., Self, S., and Mittal, T. (2019). The eruptive
961 tempo of Deccan volcanism in relation to the Cretaceous-Paleogene boundary. *Science* 363, 866-870.
962 doi.org/10.1126/science.aav1446.
- 963 Subbarao K.V. ed. (1999). “Deccan Volcanic Province”. *Geol. Soc. India Mem.* 43-1. Bangalore,
964 Geol. Soc. India, 547 p.
- 965 Swanson, D.A. (1973). Pahoehoe flows from the 1969-1971 Mauna Ulu eruption, Kilauea Volcano,
966 Hawai'i. *Geol. Soc. Amer. Bull.* 84:615-26
- 967 Swanson, D. A., DA, S., WA, D., DB, J., and Peterson, D.W. (1979). Chronological Narrative of the
968 1969-71 Mauna Ulu Eruption of Kilauea Volcano, Hawaii. Geol. Surv. U.S.A., prof. Paper; usa; da.
969 1979; no 1056; pp. 1-55; h.T. 4; bibl. 1 p.; 53 ill.; 3 cart.
- 970 Tejankar, A.V. (2002). Unpublished PhD Thesis, Study of Deccan trap flows in Toranmal ghat
971 section, Dhule district. Dr. Babasaheb Ambedkar Marathwada University,
972 <http://hdl.handle.net/10603/146932>
- 973 Thordarson, T., and Self, S. (1998). The Roza Member, Columbia River Basalt Group; a gigantic
974 pahoehoe lava flow field formed by endogenous processes? *J. Geophys. Res. B, Solid Earth and*
975 *Planets* 103, 27, 411–27,445.
- 976 Thordarson, T., and Self, S. (2003). Atmospheric and environmental effects of the 1783–84 Laki
977 eruption: a review and re-assessment, *J. Geophys. Res.* 108,4011. doi:10.1029/2001JD002042.
- 978 Vanderkluysen, L., Mahoney, J.J., Hooper, P.R., Sheth, H.C., and Ray, R. (2011) The feeder system
979 of the Deccan Traps (India): Insights from dike geochemistry. *J. Petrol.* 52, 315 – 343.
- 980 Verma, O., and Khosla, A. (2019). Developments in the stratigraphy of the Deccan Volcanic
981 Province, peninsular India. *Comptes rendus - Geosci:* <https://doi.org/10.1016/j.crte.2019.10.002>
- 982 Virtanen, P., Gommers, R., Oliphant, M., Reddy, T., Cournapeau, E., Peterson, P., Weckesser, J.,
983 Walt, M., Wilson, J., Millman, N., Nelson, A., Jones, R., Larson, E., Carey, Feng, Y., Moore, J.,
984 Laxalde, D., Perktold, R., Henriksen, I., Quintero, C., Archibald, A., Pedregosa, P., and SciPy 1.0
985 Contributors (2020). SciPy 1.0: Fundamental Algorithms for Scientific Computing in Python. *Nature*
986 *Methods* 17, 261–272.
- 987 Vye-Brown, C.L., Self, S., and Barry, T.L. (2013). Architecture and emplacement of flood basalt
988 flow fields: case studies from the Columbia River flood basalts, USA. *Bull. Volcanol.* 75, 697. DOI
989 10.1007/s00445-013-0697.
- 990 Walker, G.P.L. (1964). Geological investigations in eastern Iceland. *Bull. Volcanol.* 27(1), 351-363.

- 991 Walker, G.P.L. (1971). Compound and simple lava flows and flood basalts. *Bull. Volcanol.* 35, 579–
992 90.
- 993 Walker, G.P.L. (1999). “Some observations and interpretations on the Deccan Traps”, in *Deccan*
994 *Volcanic Province, Geol. Soc. India Memoir* 43, ed K.V. Subbarao, 367-396.
- 995 Whiteside, J.H., Olsen, P E., Kent, D.V., Fowell, S.J., and Et-Touhami, M. (2007). Synchrony
996 between the Central Atlantic magmatic province and the Triassic–Jurassic mass-extinction event.
997 *Palaeogeography, Palaeoclimatology, Palaeoecology* 244(1-4), 345-367.
- 998 Xu, Y., et al. (2018) Paleomagnetic secular variation constraints on the rapid eruption of the Emeishan
999 continental flood basalts in southwestern China and northern Vietnam. *J. Geophys. Res.: Solid Earth*
1000 123.4, 2597-2617.

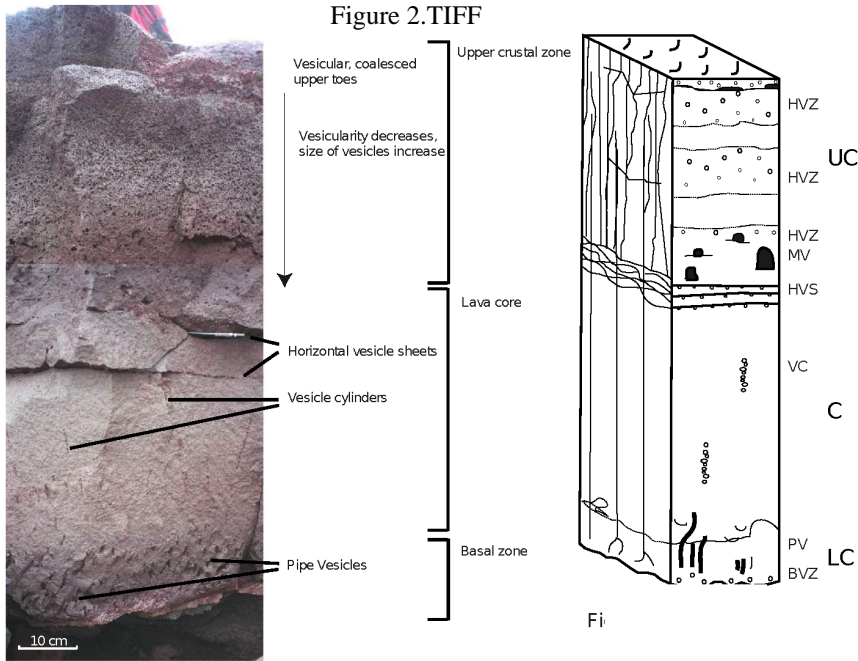
In review

Figure 1.TIF



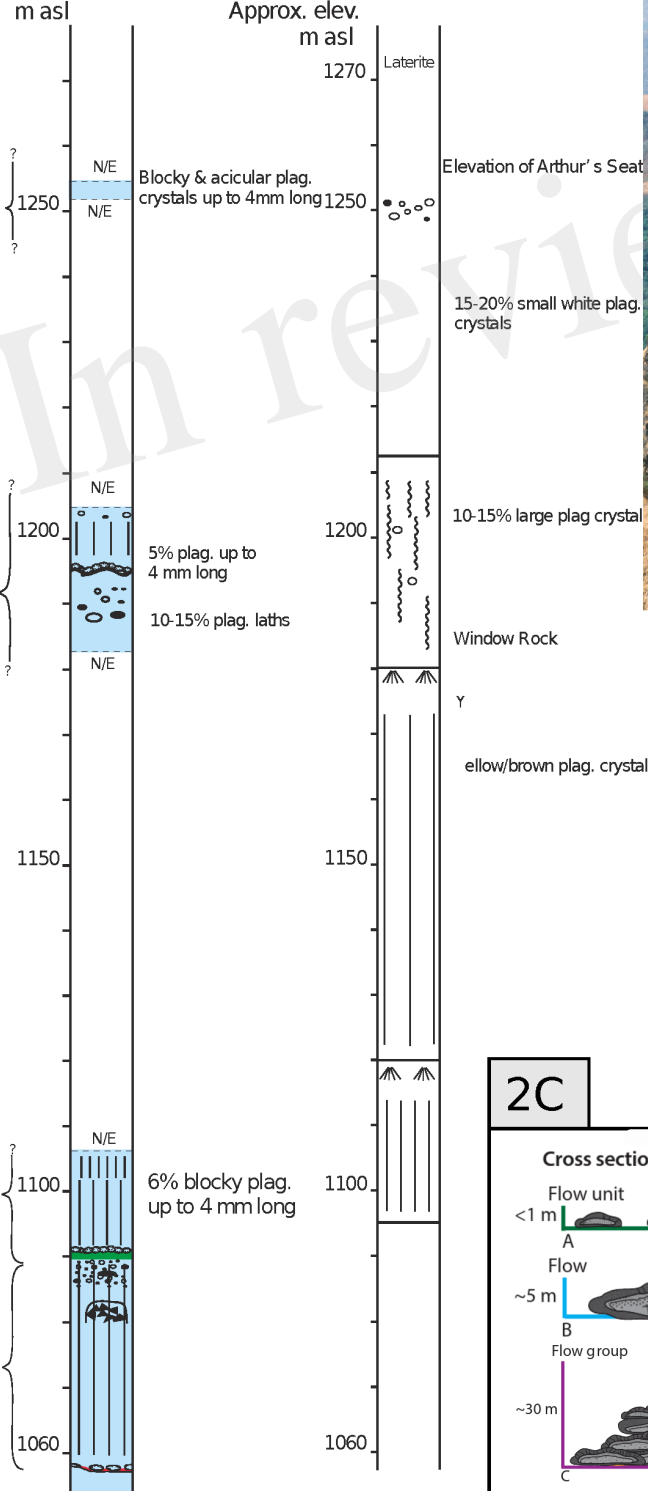
2A

Figure 2.TIFF

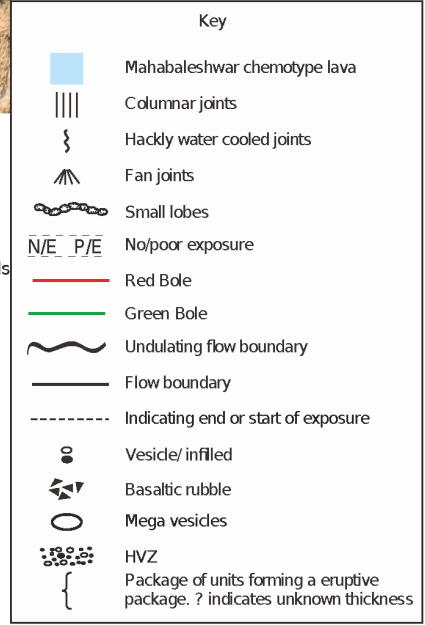


Ambenali Ghat

Arthur's Seat



2B



2C

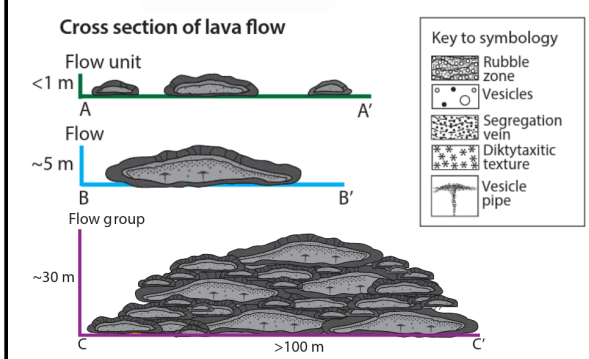
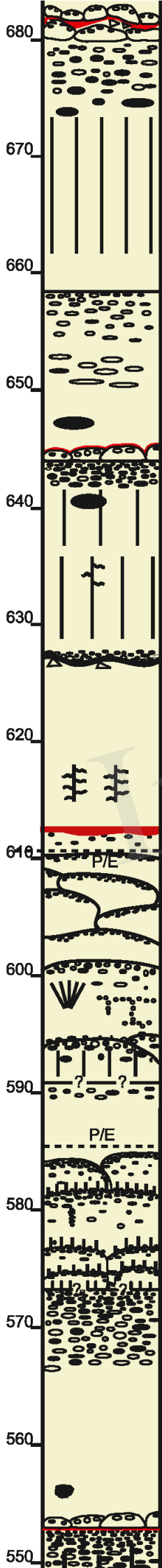


Figure 3.TIFF

3A

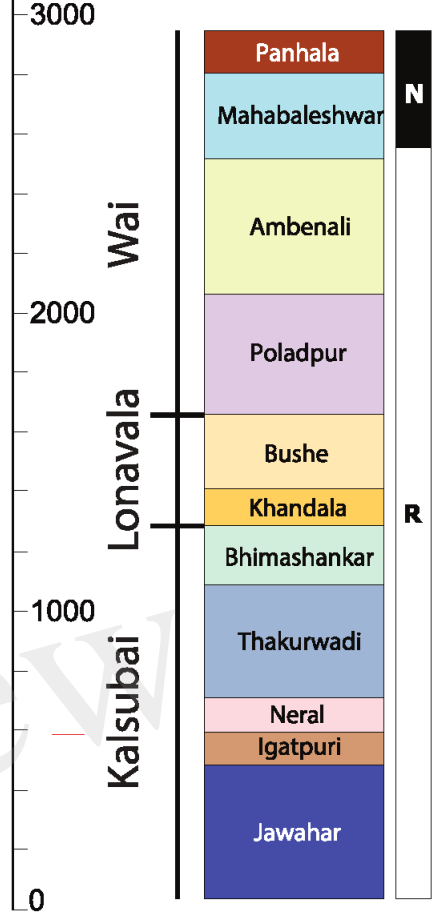
3B



Key

- △△ Rubbly blocks
- |||| Columnar joints
- }}} Hackly joints
- ⊥⊥ Perpendicular joints
- ⊙ Radial joints
- ||| Pipe vesicles
- ⊙ Vesicles
- ⊙ Amygdales
- ⊙ Mega vesicles
- ⊙ Vesicular patches
- HVS
- ⊙ Vesicle cylinders
- Small break-out or precursor lobes
- Thin stacked lobes
- eruptive package of unknown size
- Flow boundary
- Undulating flow boundary
- Lobey flow top
- ?-?-? Poorly visible or suspected flow boundary
- Bole or red weathering horizon
- Red bole on undulating flow top
- Ambenali Formation
- Reversely magnetised
- P/E Poor exposure

Stratigraphic thickness in m



3C

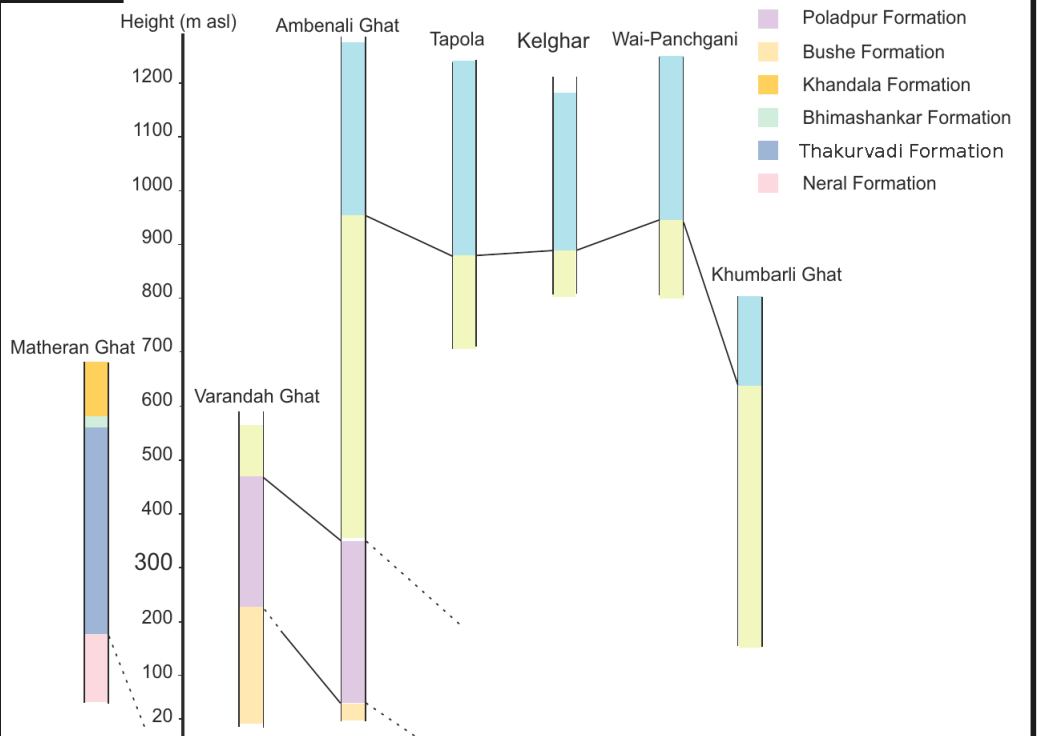
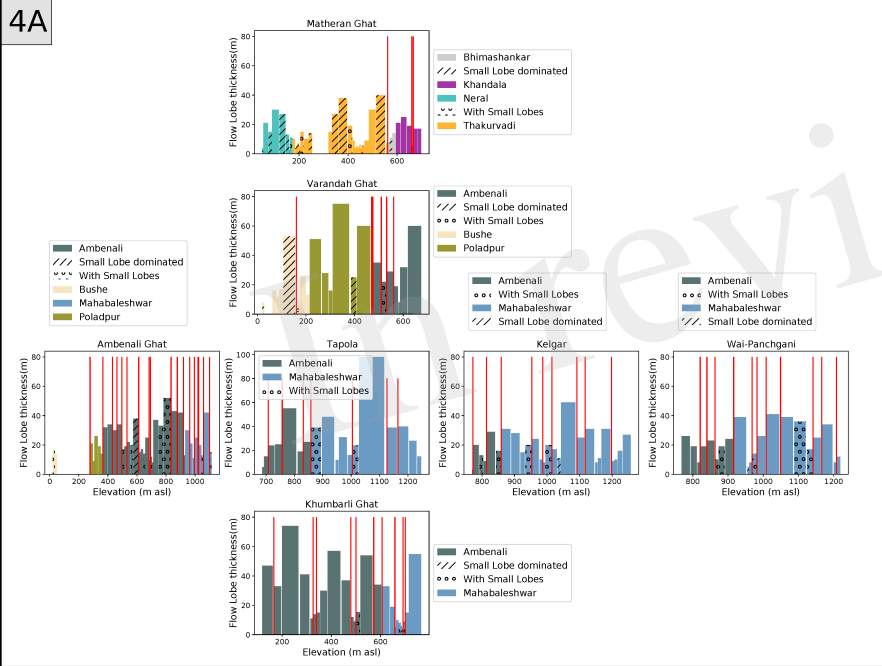


Figure 4.TIF

4A



4B

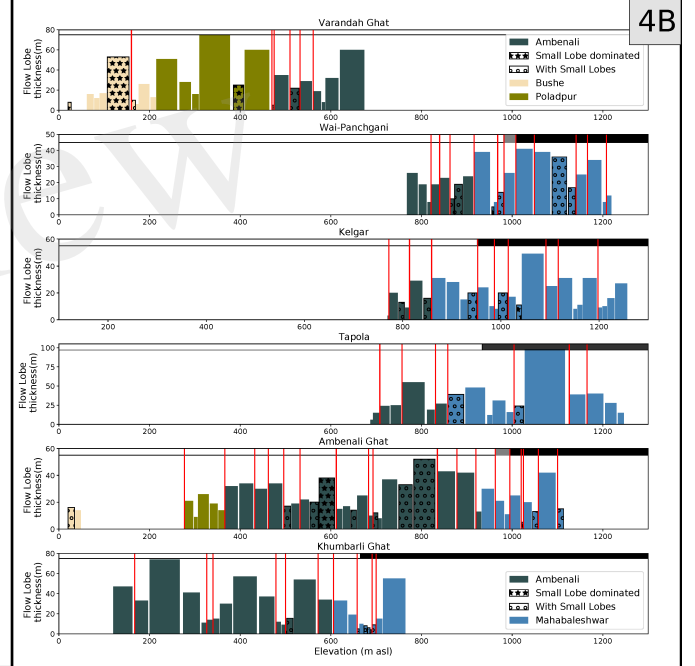
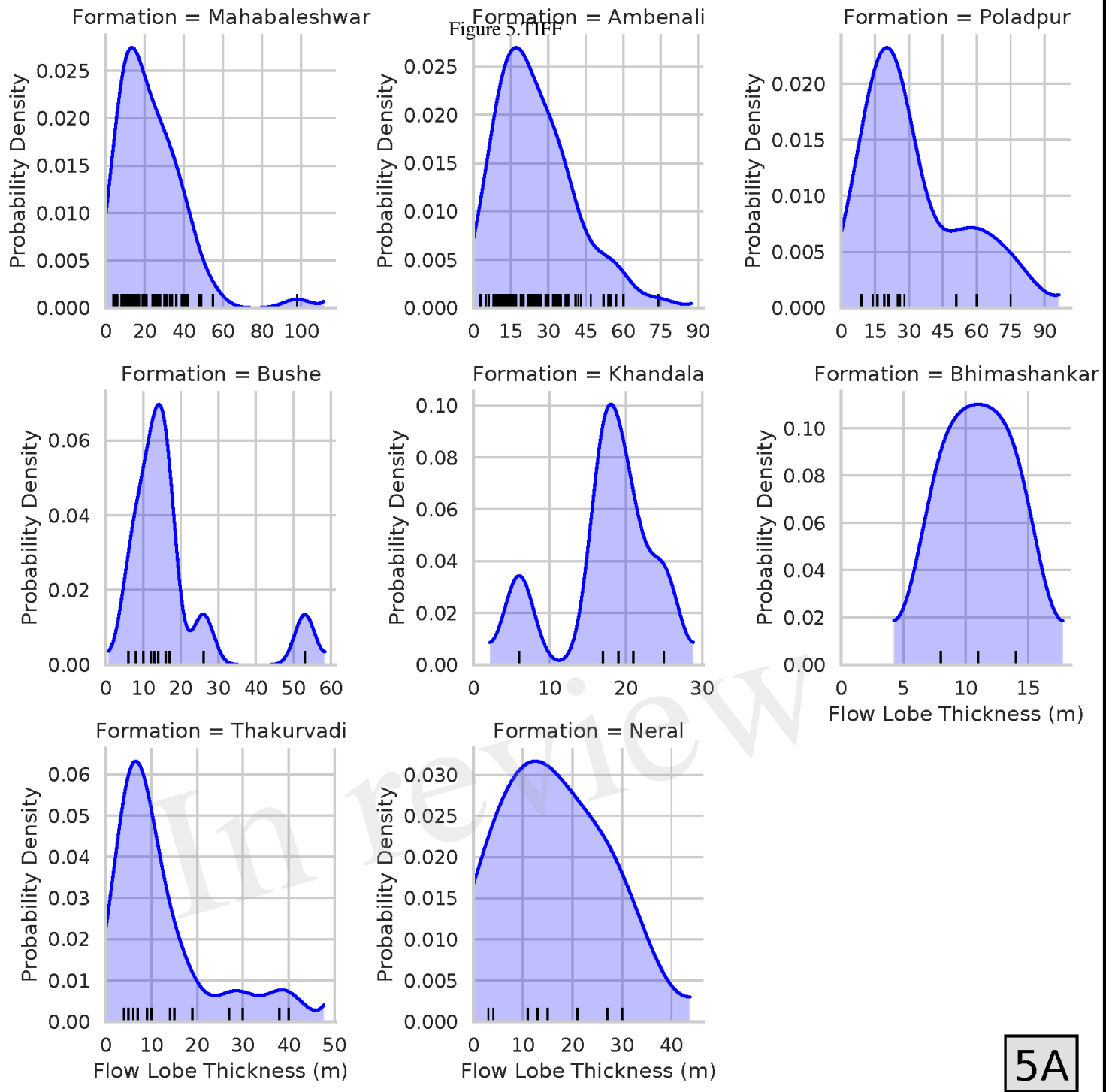
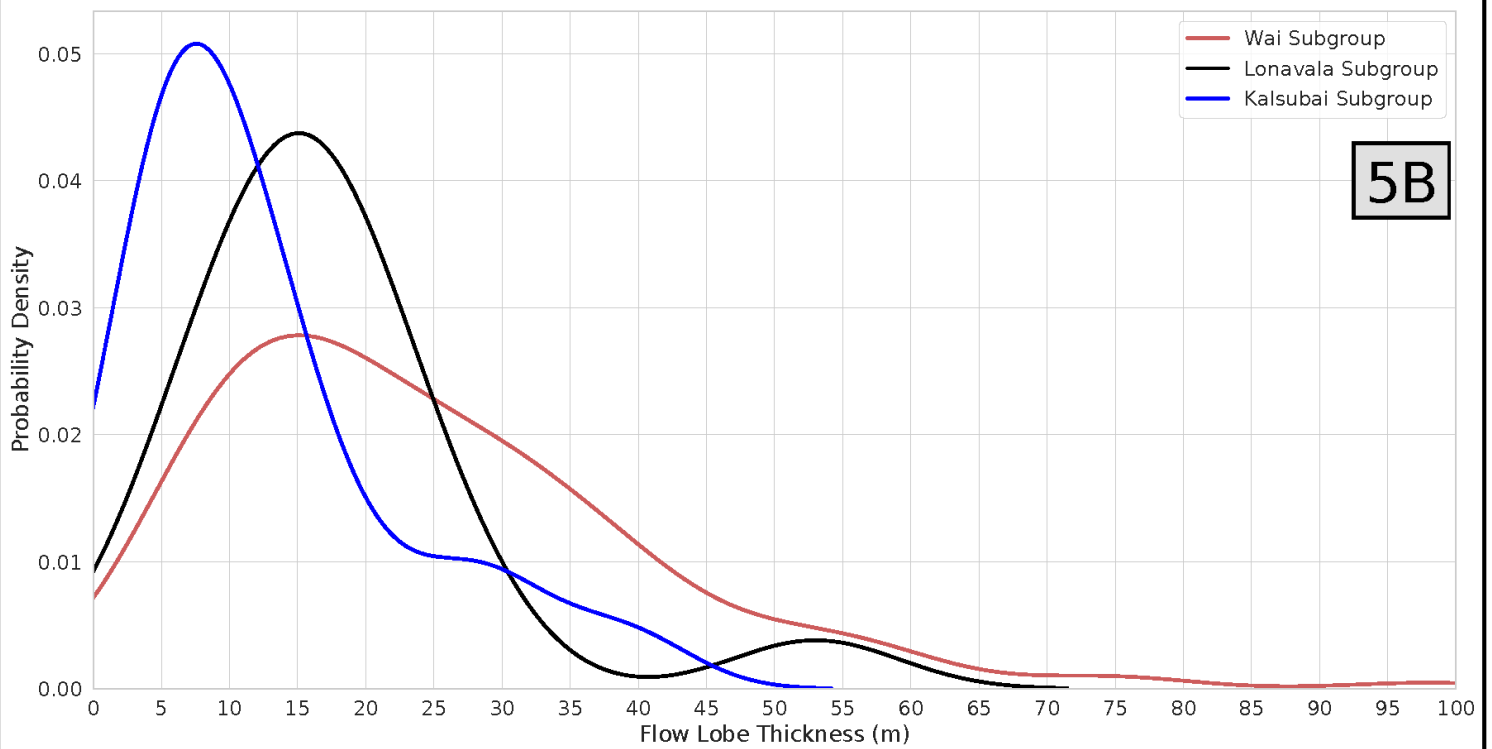


Figure 5.11F



5A



5B

Figure 6.TIFF

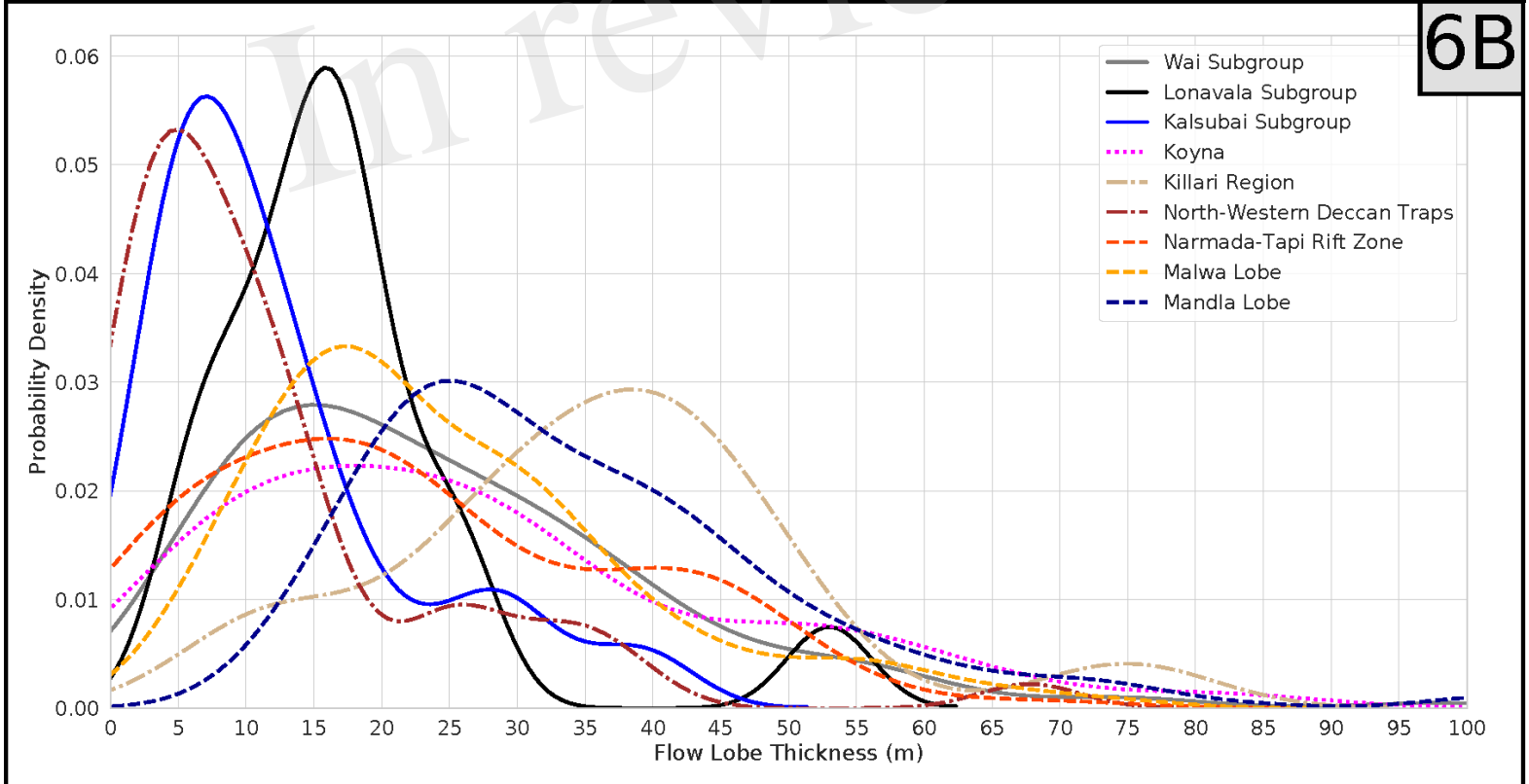
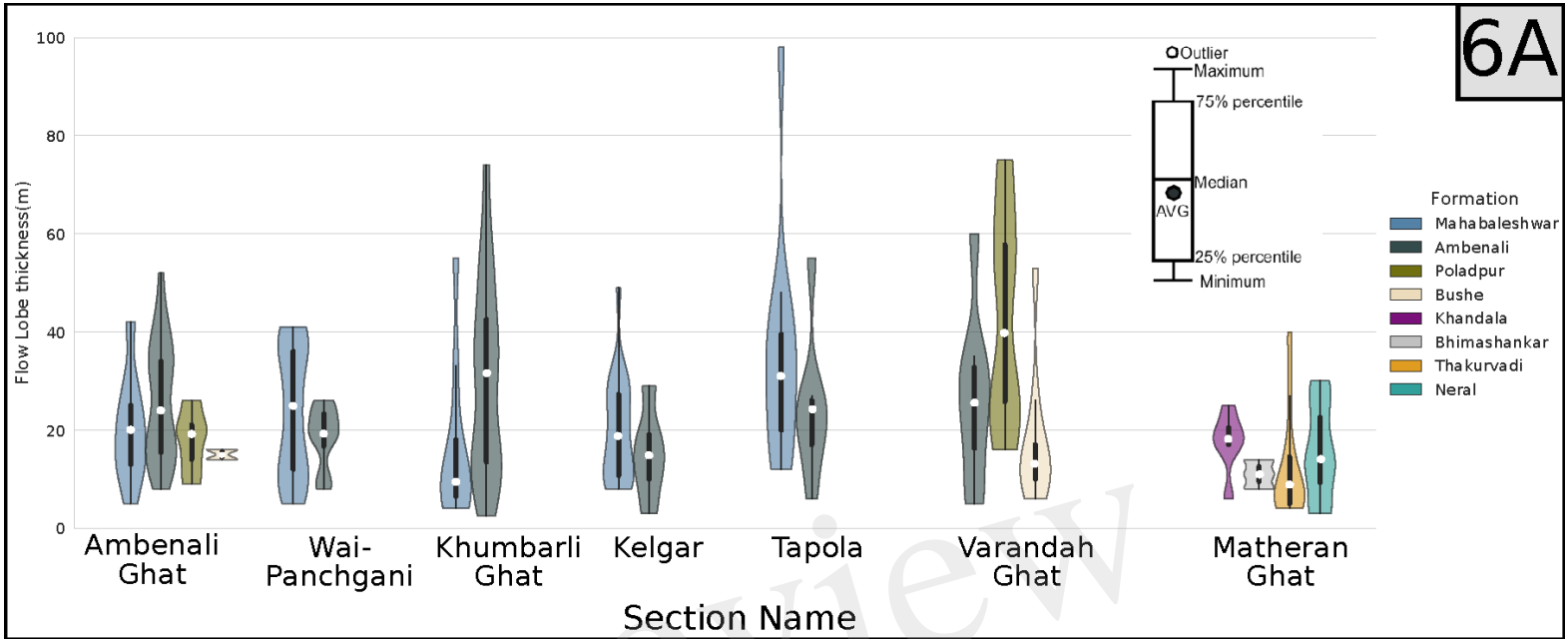
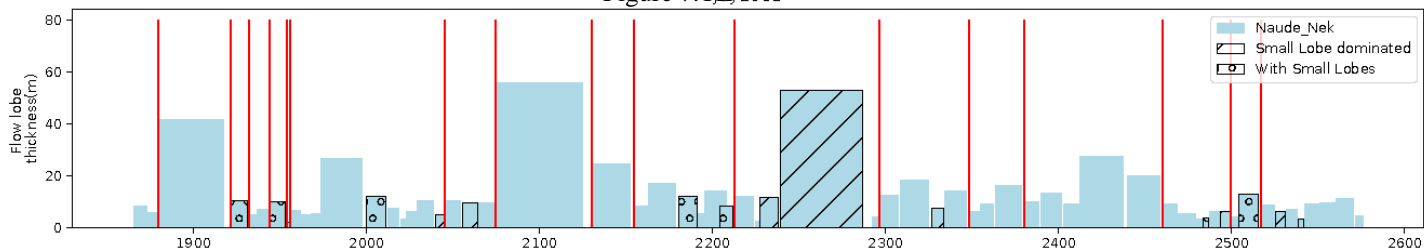
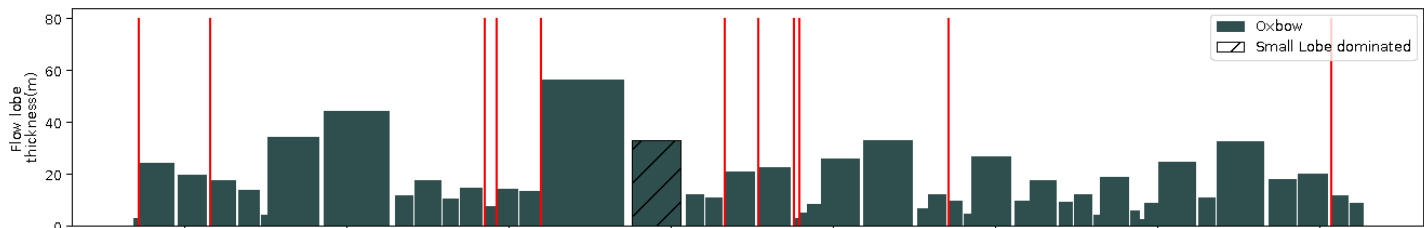


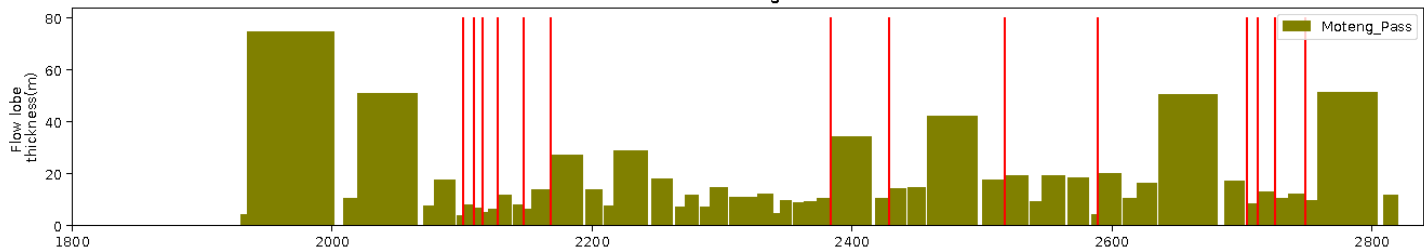
Figure 7. TB 2018



Moulin2017



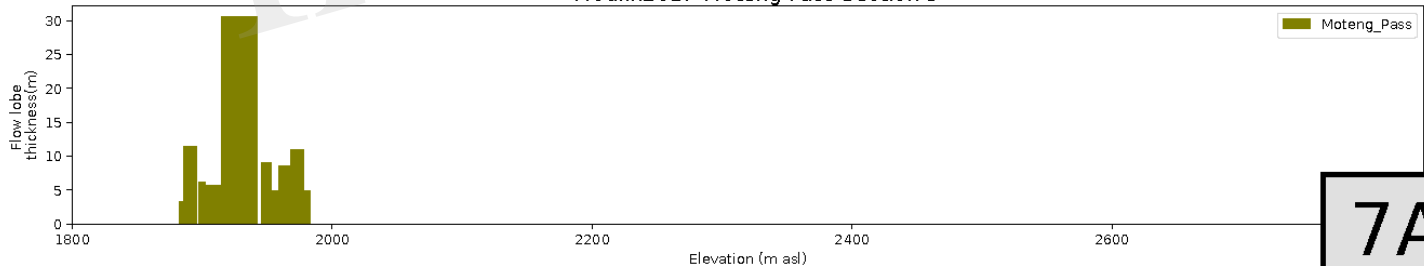
Moulin2017 Moteng Pass Section 1



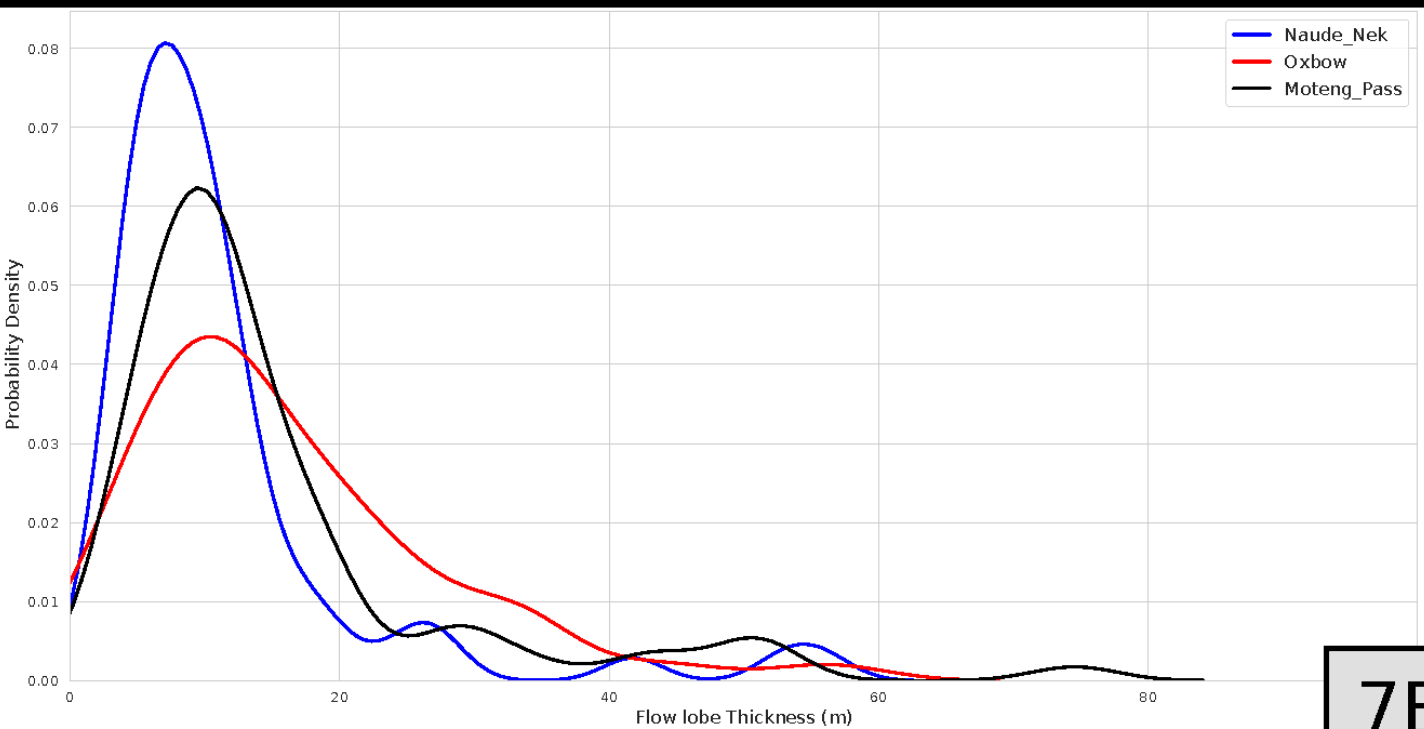
Moulin2017 Moteng Pass Section 2



Moulin2017 Moteng Pass Section 3



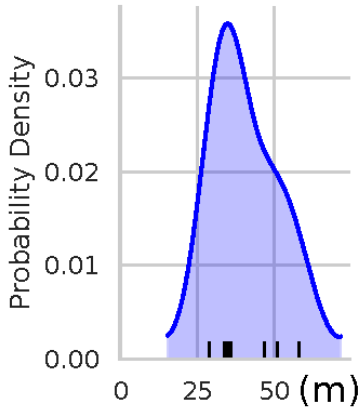
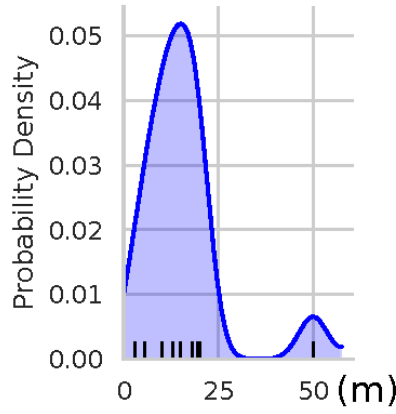
7A



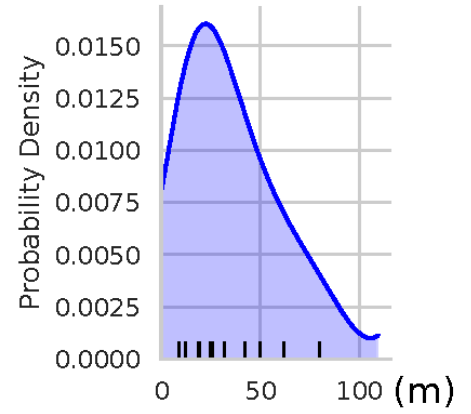
7B

8A

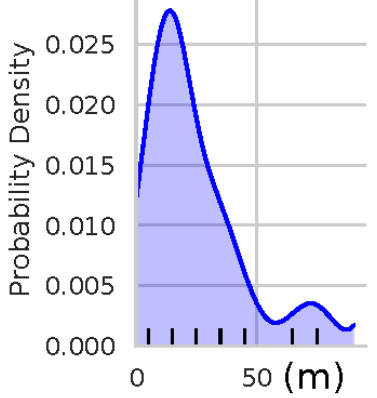
Location = Palouse Falls

Figure 8.TIF
Location = Ginkgo

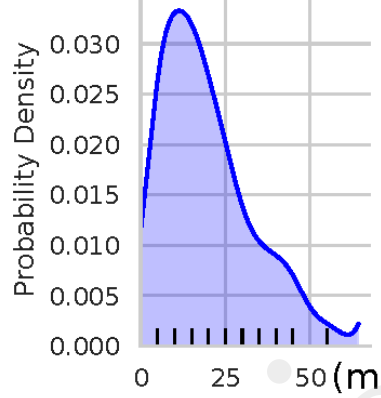
Location = Sand Hollow



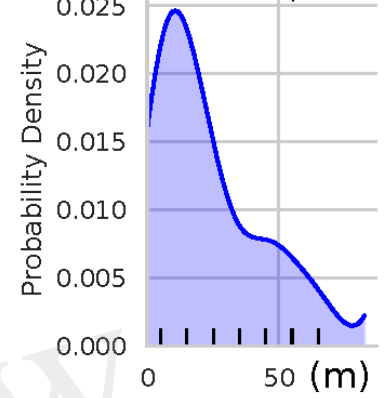
Location = Wanapum (unpub)



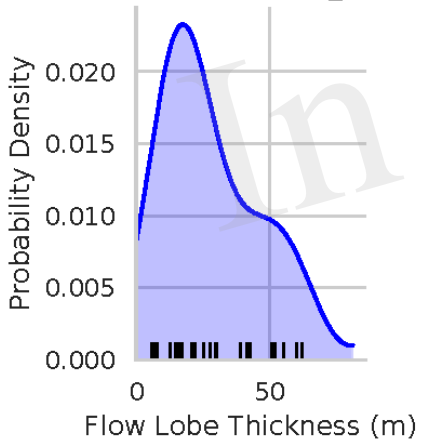
Location = Roza



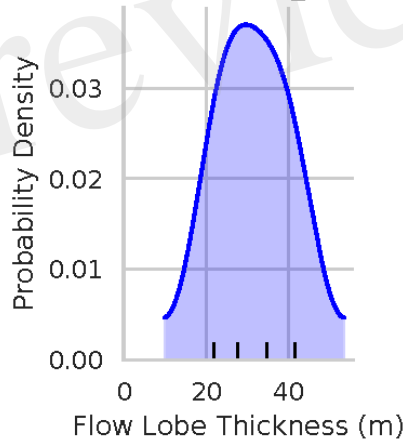
Location = Grande Ronde (unpub)



Location = Grande_Ronde



Location = Wallula_Wanapum



Location = Steens Mountain

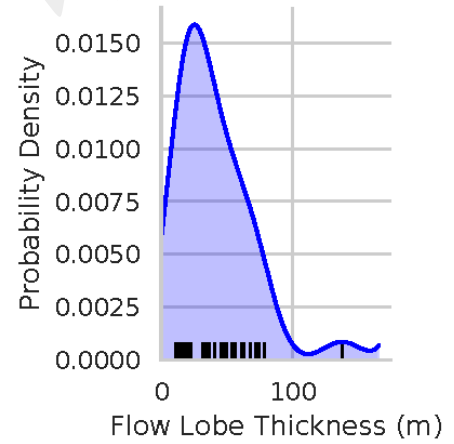
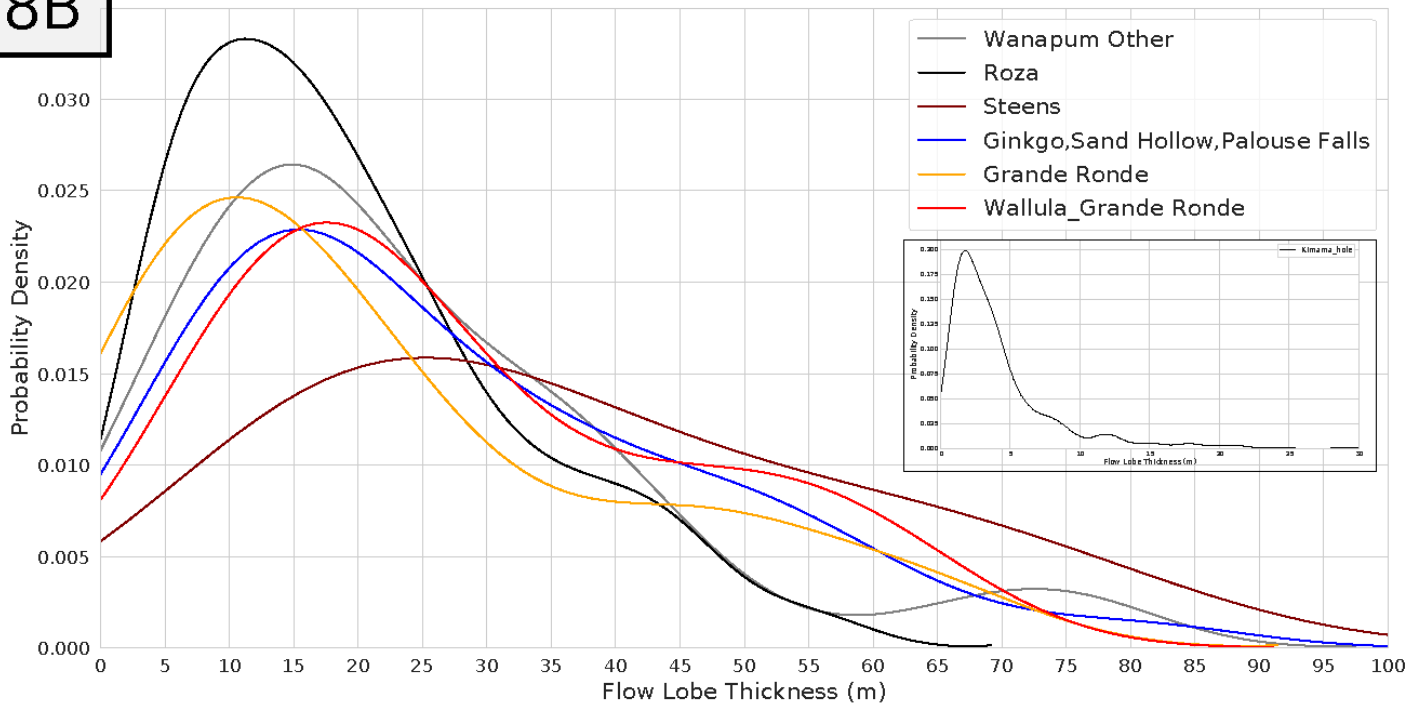
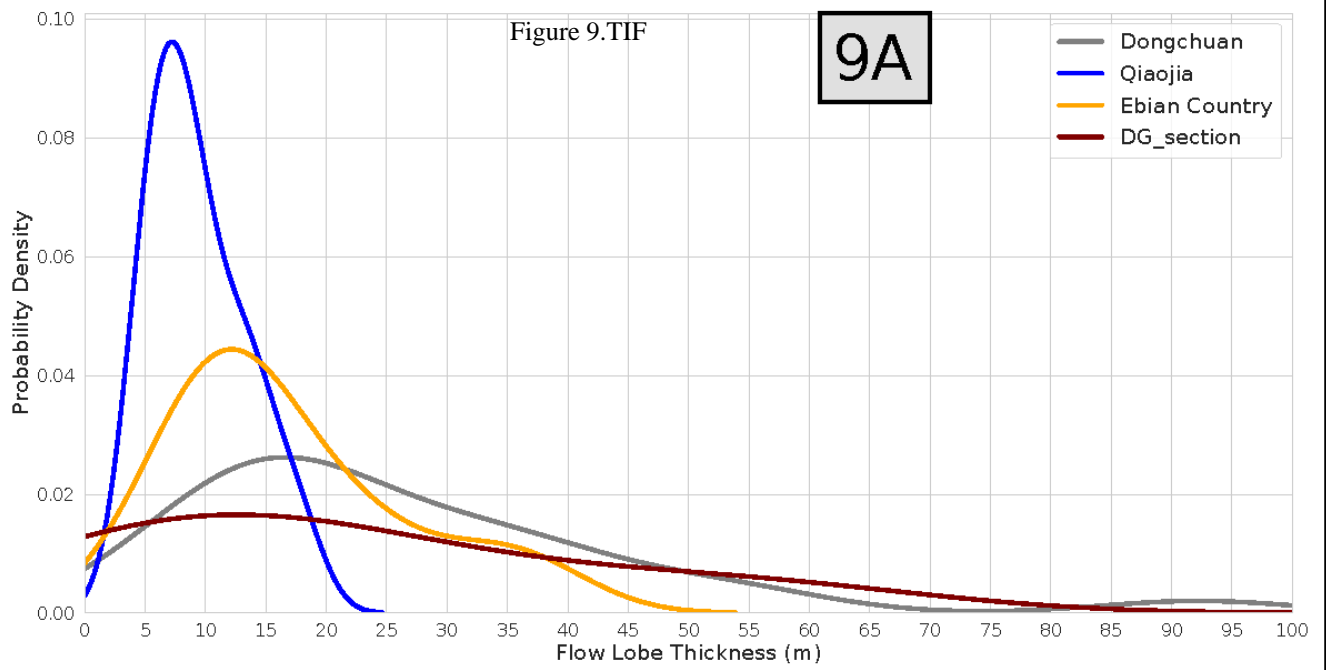
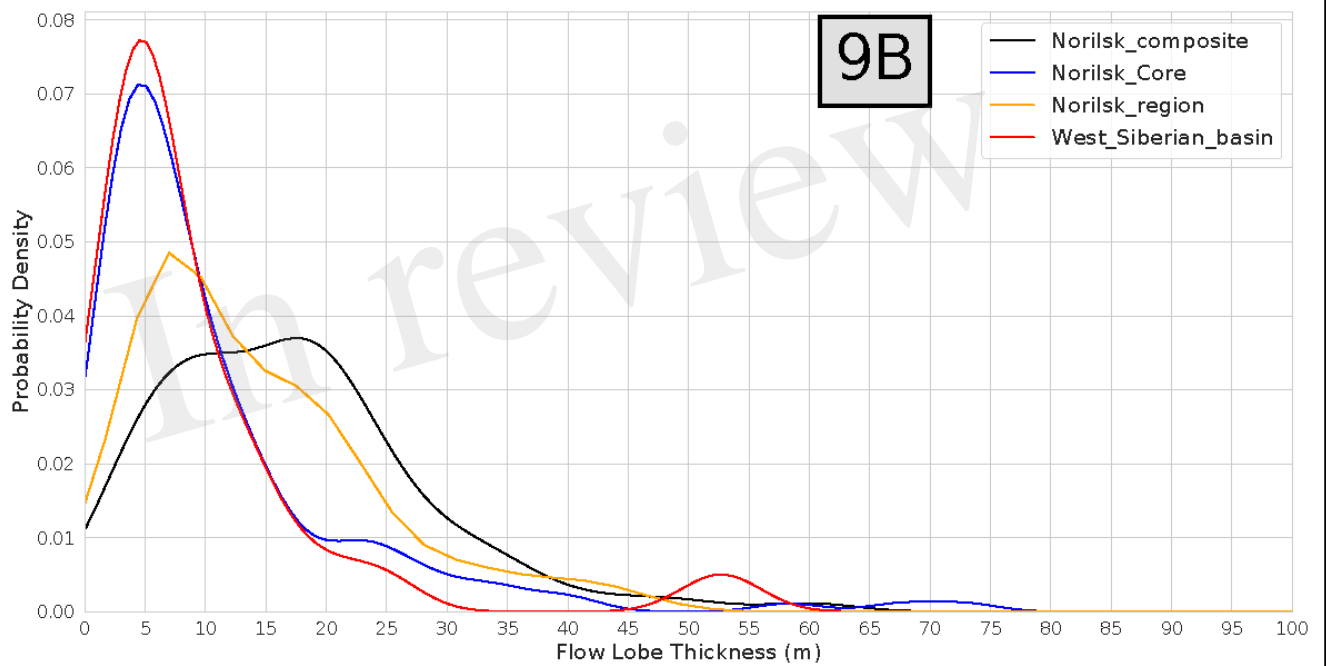
**8B**

Figure 9.TIF

9A



9B



9C

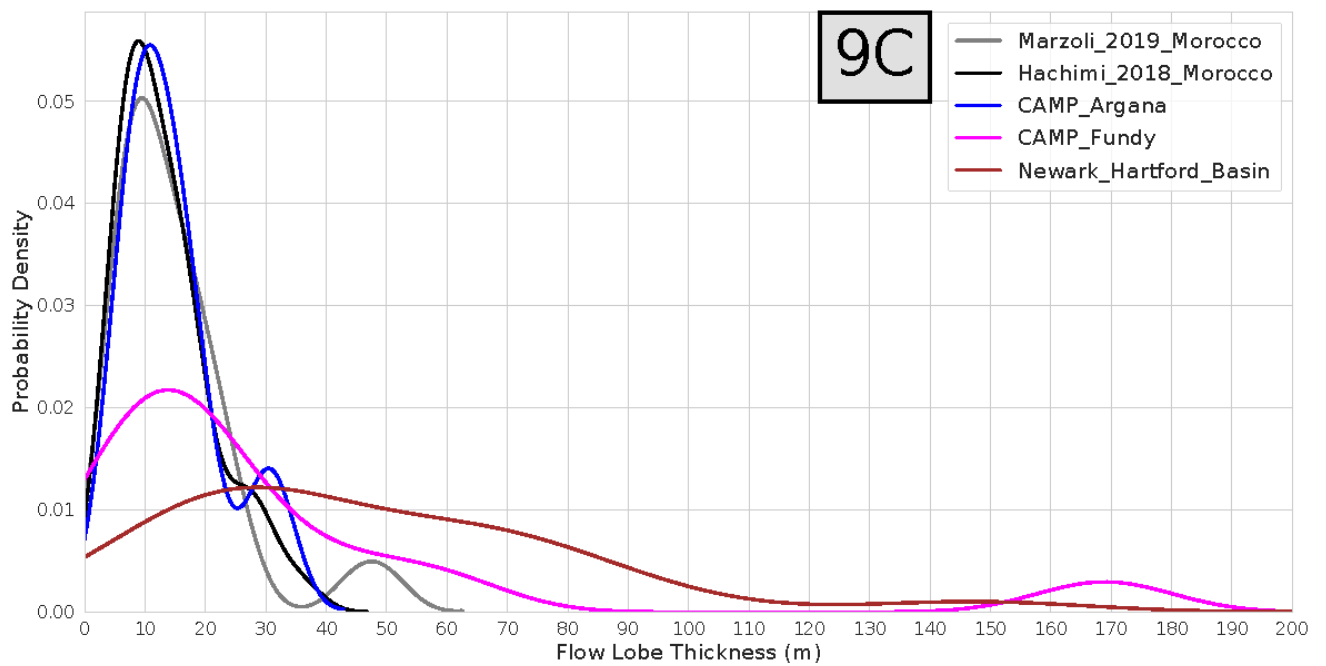
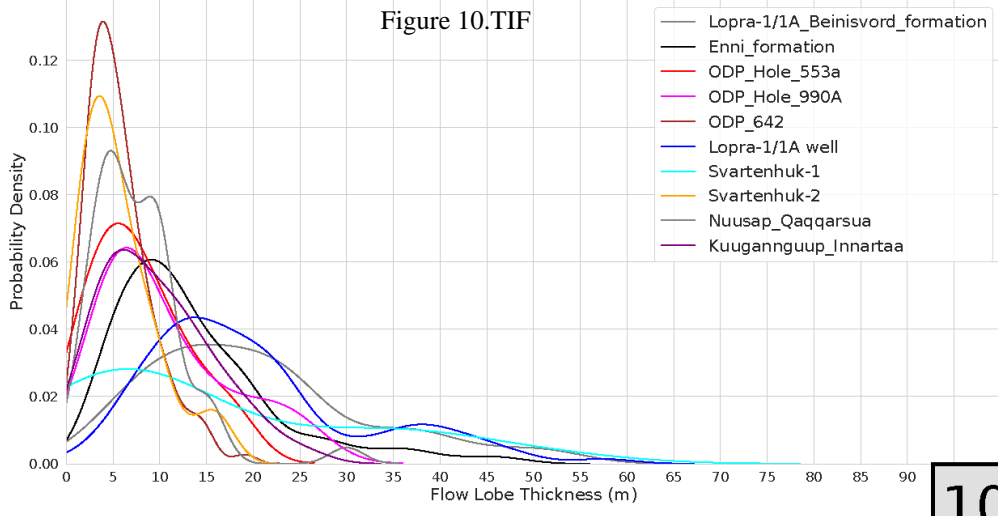
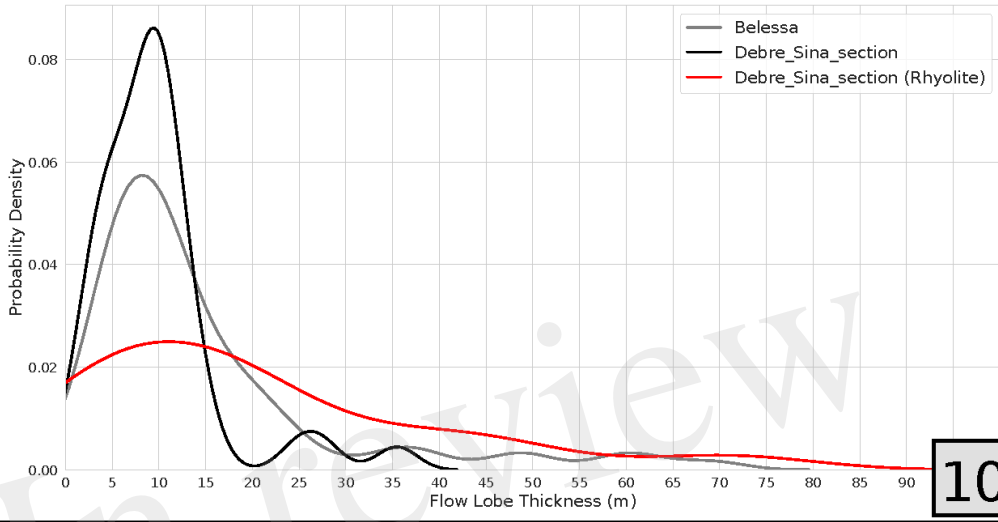


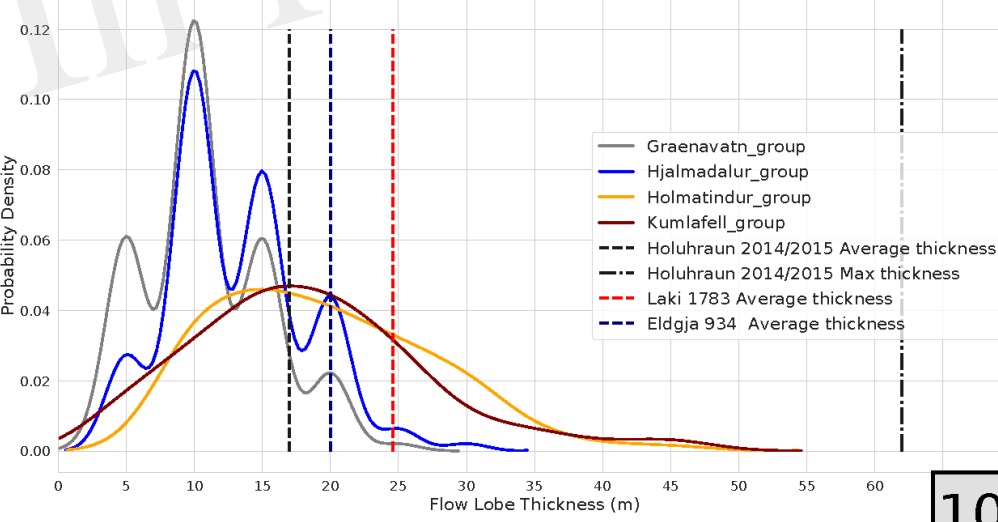
Figure 10.TIF



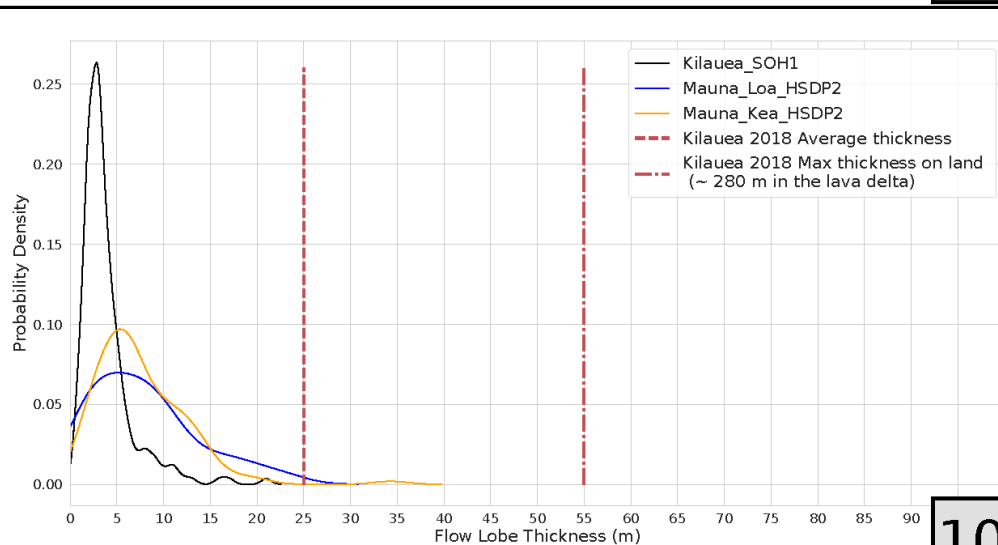
10A



10B

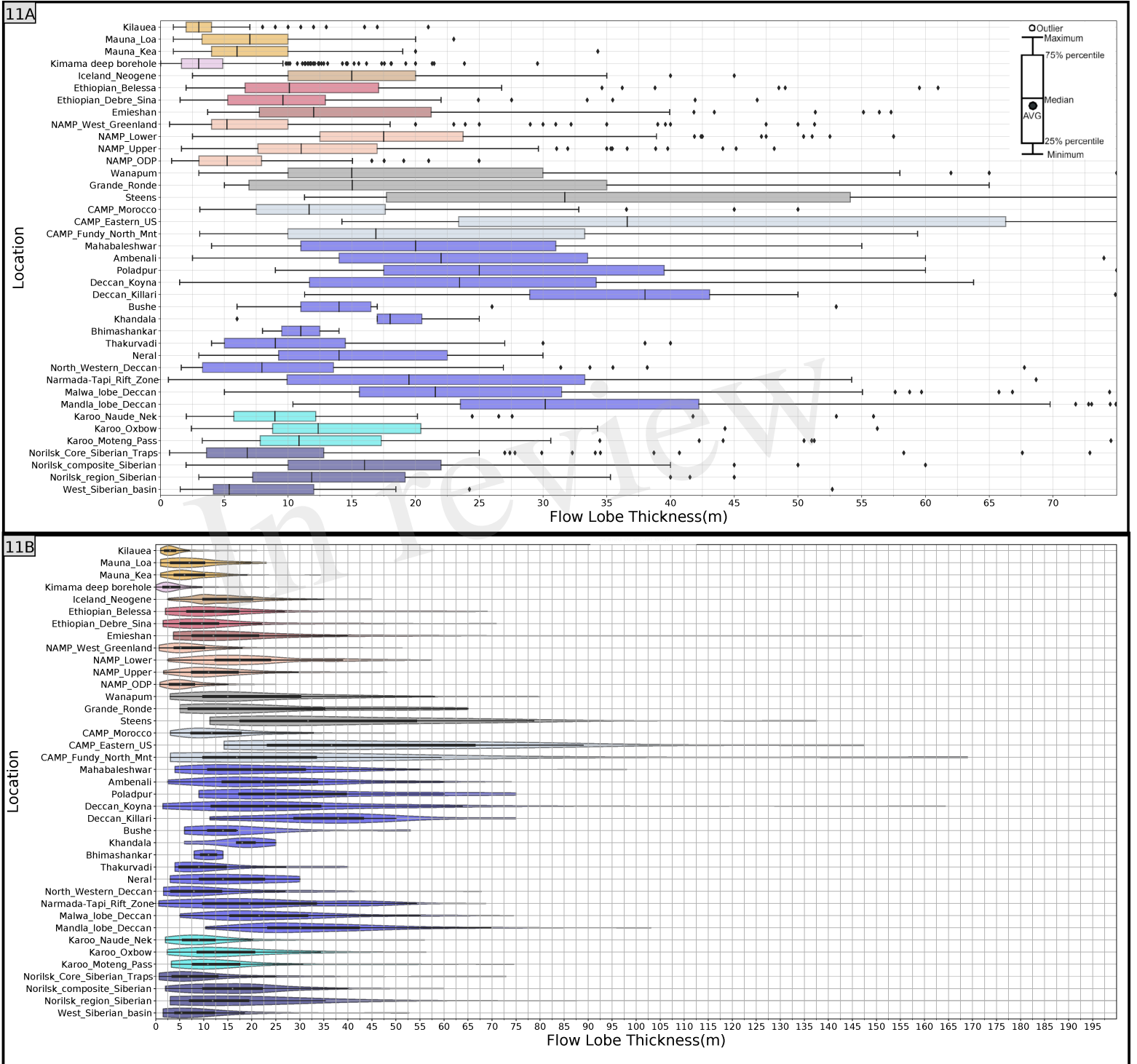


10C



10D

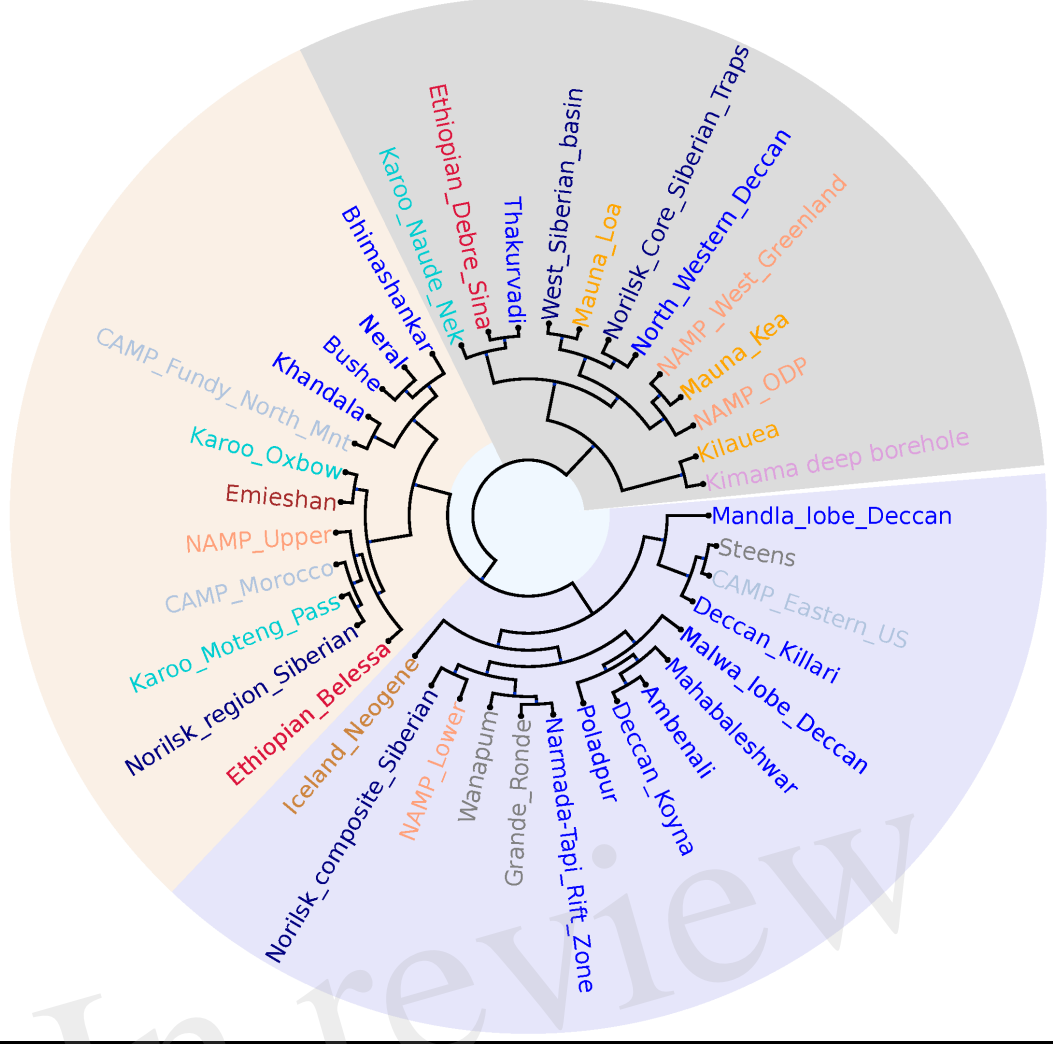
Figure 11.TIF



12A

Anderson-Darling Test Classification

Figure 10.THF



12B

Epps Singleton Test Classification

